How Extreme Apparitions of the Anthropogenic West African Aerosol Plume cause Drought in the Iberian Peninsula, Floods in the U.K. and Ireland and higher winter temperatures in Northern Europe. First Attribution and Mechanism using data from the Terra Satellite, Last Millennium Ensemble, and the MERRA-2 and NCEP/NCAR Reanalyses.

K. A. Potts[1]

[1] Kyna Keju Pty Ltd.

Corresponding author: Keith Potts (Keith.Potts@bigpond.com)

Key Points:

- Winter droughts in the Iberian Peninsula are caused by extreme apparitions of the anthropogenic West African aerosol Plume (WAP).
- Simultaneously the WAP also causes winter floods in the U.K. and Ireland and higher winter temperatures in northern Europe.
- The WAP creates these effects by perturbing the location of the northern regional Hadley Circulation from late December to early April.

Abstract

The literature, Inter Governmental Panel on Climate Change (IPCC) and the USA Climate Change Science Program suggest that aerosols can affect the large-scale atmospheric circulation and hydrologic cycle I therefore examine the relationship between aerosols and Iberian droughts, floods in the UK/Ireland and higher European winter temperatures. Aerosols exist mainly as eight continental scale plumes which typically, but not exclusively, exist for a few months in the tropics at the end of the local dry season when biomass burning can occur. The anthropogenic West African aerosol Plume (WAP) exists from late December to early April and is located in the region which drives the northern regional Hadley Circulation towards Europe. It is therefore the prime candidate for investigation into European, winter climate variability. Using the Last Millennium Ensemble (1,156 years and 13,872 months of data) and the MERRA-2 reanalysis (40 years of data) I show that drought in the Iberian Peninsula, floods in the UK/Ireland and higher winter temperatures in northern Europe are created by extreme apparitions of the anthropogenic WAP. The WAP creates these effects by Aerosol Regional Dimming (ARD), which, by altering the surface radiation budget under the plume and warming the upper atmosphere, forces the regional Hadley Circulation into an abnormal seasonal position. These effects alter the regional atmospheric circulation systems and hydrologic cycle in Europe thereby causing drought, floods and higher temperatures and, as the WAP has intensified over recent decades, created climate change.

Plan Language Summary

The West African aerosol plume, one of eight continental scale aerosol plumes (https://www.essoar.org/doi/10.1002/essoar.10500075.1), is shown to change the atmospheric circulation systems between West Africa and Europe which creates anomalous, persistent high pressure over the Mediterranean and Iberia. This high pressure forces the winter storms crossing the Atlantic to the north and creates drought in Iberia. The high pressure also creates a persistent south westerly air flow from the central Atlantic into Europe north of the Alps, the UK and Ireland. Coming from further south this air flow is warmer than is usual in this season and this raises the winter temperature in Europe. The airflow is also carrying higher levels of moisture as it originates over warmer seas and, as it reaches the UK and Ireland, it has cooled enough to release this extra moisture as rain resulting in floods in these countries.

Hence significant changes in the winter climate in Europe north of the Alps, the UK, Ireland and Spain are caused by the West African aerosol plume and action should be taken immediately to eliminate the plume and which will return the winter climate of Europe to its natural state circa 1950.

1 INTRODUCTION

1.1 HYPOTHESIS AND PHYSICAL MODEL

van Oldenborgh et al. [2009] state that “the observed temperature rise around 52_ N is dominated by circulation changes.” and that “a significant increase in air pressure over the Mediterranean (Osborn, 2004) (z>3) and a not statistically significant air pressure decrease over Scandinavia (z<2) have brought more mild maritime air into Europe north of the Alps.”

This paper therefore explores an explicit physical model and hypothesis to explain how the West African aerosol Plume (WAP) causes the “significant increase in air pressure over the Mediterranean” which simultaneously creates higher European winter temperatures, drought in the Iberian Peninsula and floods in the UK and Ireland. The sequence of events is:

1. The anthropogenic aerosol plume forms over West Africa in late December and dissipates in early April with the start of the West African monsoon;
2. The aerosols absorb (and reflect) solar radiation which heats the atmosphere;
3. The aerosols reduce the solar radiation at the surface under the plume which cools the surface;
4. 2 and 3 create a temperature inversion compared to times without a plume and this reduces convection in the region;
5. The region to the north of the WAP is now the driving force of the convective leg of the northern regional Hadley Cell;
6. This northerly move in convection perturbs the entire northern Hadley Cell;
7. This results in higher pressure over the Mediterranean Sea and the Iberian Peninsula;
8. This forces the cold fronts crossing the Atlantic north and reduces winter rainfall over the Iberian Peninsula;
9. The high pressure over the Mediterranean Sea and Iberian Peninsula advects warm, moist air from the central Atlantic Ocean into northern Europe
10. This raises the winter temperature in northern Europe; and
11. Introduces increased levels of moisture into the U.K. and Ireland and causes floods.

1.2 Pressure over the Mediterranean and the Iberian Peninsula

There has been a significant increase in sea-level pressure over the Mediterranean Sea and the Iberian Peninsula in the winter months in recent decades as Figure 1, which recreates part of Figure 7 in [*van Oldenborgh et al.*, 2009] from the NCEP/NCAR reanalysis [*Kalnay et al.*, 1996], shows. In Assessment Report 5 (AR5) the IPCC noted: “Changes in atmospheric circulation are important for local climate change because they could lead to greater or smaller changes in climate in a particular region than elsewhere. It is likely that human influence has altered sea level pressure patterns globally.”. This is exactly what this paper demonstrates: that the anthropogenic WAP creates the increase in pressure over the Mediterranean and Iberia and it, in turn, drives the changes in the winter climate of Europe.

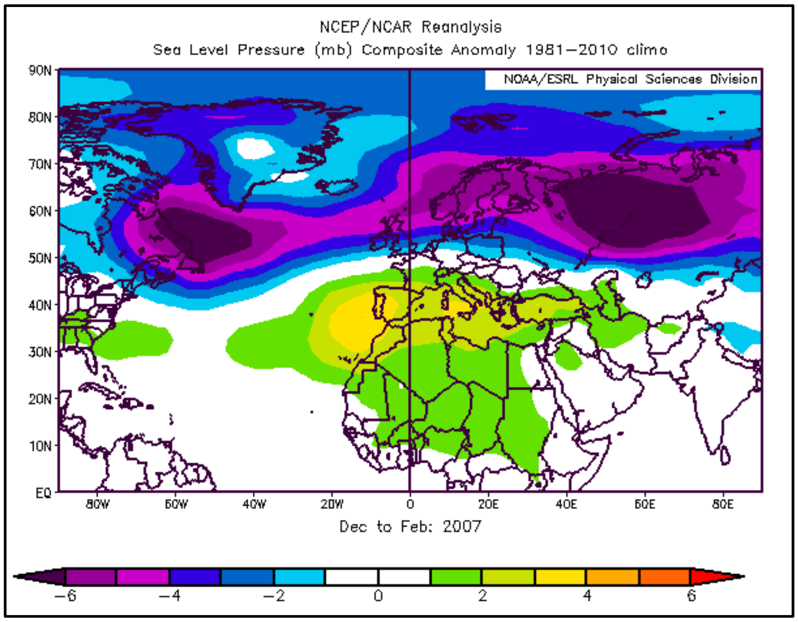

Figure 1: NCEP/NCAR Sea-Level Pressure anomaly (Dec to Mar 2007). Note the period of the NCEP climate average is now 1981 to 2010.

1.3 Drought in Spain

García-Herrera et al. [2007] identified “an impressive northward displacement of cyclone trajectories in the North Atlantic sector in winter months resulting in an almost complete absence of cyclones crossing Iberia and western Europe.” as a significant driver of the 2004/05 hydrological year drought in Iberia and noted that “The results obtained within this work show the [North Atlantic Oscillation] NAO and [East Atlantic] EA indexes, two of the most prominent North Atlantic teleconnection patterns modulating climate in the Iberian Peninsula, incapable to detect the low precipitation totals in March.”

Vicente-Serrano and López-Moreno [2006] investigated the relationship between the occurrence of drought in NE Spain and atmospheric circulation and found an increase in the number of anti-cyclonic days in winter from 1950 to 2000 which results in lower rainfall in NE Spain. Figure 5 in the paper shows Spain covered by higher than average pressure in winter during these days.

Trends in sea-level pressure in Europe are shown in *van Oldenborgh et al.* [2009] in Figure 7 from 1950–2007 using the NCEP/NCAR reanalysis which show a significant increase in pressure over Iberia and the Mediterranean. Comparisons of observed changes and climate model simulations are also included and the paper states: “In Fig. 7 of the paper trends in sea-level pressure over 1950–2007 of the NCEP/NCAR reanalysis are compared to climate model simulations. Both the reanalysis and the ESSENCE ensemble show a significant trend in the Mediterranean region, but the observed trend is a factor four larger than the modelled trend. The GFDL CM2.1 and MIROC 3.2 T106 models also show significant positive trends in this area, but again much smaller than observed. The other two models show no positive trends there.” Details of the ESSENCE ensemble are provided in [*Sterl et al.*, 2008] which shows that in the historic data only tropospheric sulphate aerosols are included and the ESSENCE ensemble cannot therefore have modelled the WAP correctly as it is predominantly composed of carbonaceous aerosols (Appendix A).

This paper demonstrates why such an increase in sea-level pressure has occurred over Iberia in winter in recent decades and therefore why the peninsula has endured an increased frequency of drought.

1.4 Floods in the United Kingdom

The United Kingdom (UK) has experienced significant floods in winter in recent decades with 2002, 2005, 2009, 2010, 2012, 2014, 2015, 2019 and 2020 noted as significant rainfall/flood events on the UK Met. Office website at https://www.metoffice.gov.uk/weather/learn-about/past-uk-weather-events demonstrating a return frequency of just over 2 years. As I write in February 2020 storms Ciara and Dennis have just unleashed more UK and Irish floods.

In the winter of 2013-14 a rapid succession of Atlantic low pressure systems crossed the UK with large increases in rainfall in the south of England and much of Scotland [Huntingford et al., 2014] who noted "The role of anthropogenic aerosol effects requires further work, especially on tropical atmospheric circulation and hence rainfall, given high regional variations in concentration of aerosols compared with well-mixed GHGs". This is the focus of this paper.

Schaller et al. [2016] also investigated the 2014-15 floods using a regional climate model covering the UK and eastern North Atlantic Ocean to investigate the effects of anthropogenic emissions on the winter climate of the UK. However, the only mention of aerosols in the paper refers to "sulphate aerosol precursors" and it cannot therefore have included the carbonaceous aerosols which constitute the WAP which this paper addresses. They did note "More studies of this nature are needed if loss and damage from anthropogenic climate change are to be quantified objectively and future assessments of the impacts of climate change are to progress from attributing them simply to changes in climate which are not themselves explained, to attributing them specifically to human influence." Which, again, is exactly what this paper does.

1.5 Higher Winter Temperatures in Northern Europe

The IPCC has identified Europe as one of the fastest warming regions of the world and in Assessment Report 4 (AR4) discussing changes since 1979 stated: "Warming in this period was strongest over western North America, northern Europe and China in winter". IPCC AR5 states "Regardless of whether the statistics of flow regimes themselves have changed, observed temperatures in recent years in Europe are distinctly warmer than would be expected for analogous atmospheric flow regimes in the past, affecting both warm and cold extremes citing [*Yiou et al.*, 2007] and [*Cattiaux et al.*, 2010]"

The European winter of 2006-07 was exceptionally warm and the New Scientist reported that "the temperatures experienced during autumn 2006 and winter 2007 are likely to have been the warmest in 500 years, they say. But the sequential combination of two such warm seasons is a still rarer event - probably the first since 1289" citing *Luterbacher et al.* [2007]. *van Oldenborgh et al.* [2009], based on *Osborn* [2004], states the winter temperature rise in Europe is dominated by circulation changes that bring mild maritime air into Europe north of the Alps and, as noted above, climate modelling fails to replicate these circulation changes – specifically the higher pressure over the Mediterranean Sea and Iberia.

Osborn [2004] used an ensemble of seven climate models and observations to analyse the significance of the trend noting: "An improved understanding of past precipitation would help towards improved regional-scale projections of the future, which are of huge value to policymakers."

Figure 1 from the NCEP/NCAR reanalysis dataset shows the high-pressure anomaly discussed by [*van Oldenborgh et al.*, 2009]. Such an area of persistent high-pressure over the Mediterranean Sea advects warm air from the central Atlantic to northern Europe resulting in anomalously high temperatures as noted by *van Oldenborgh et al.* [2009]

These cited papers suggest that the climate modelling which was reviewed does not include the forcing agent which caused the rise in pressure over the Mediterranean and Iberia which this paper shows to be the carbonaceous, anthropogenic WAP.

1.6 Aerosols and Climate

The IPCC Assessment Report 4 (AR4) [*Solomon et al.*, 2007] identifies the two main anthropogenic contributors to climate change as Long Lived Green House Gases (LLGHG) and aerosols and defines Radiative Forcing (RF) as the global annual average of "the change in the net, downward minus upward, irradiance (expressed in W m^{-2}) at the tropopause". The IPCC AR4 also discusses Surface Forcing (SF), the effects of the forcing agents at the surface of the Earth and Figure 2 from that report shows the evolution of RF and SF from 1850 to the present day. It can be clearly seen that the net anthropogenic RF effect, black line – panel (A), follows the red line of LLGHG reasonably closely. However, the net anthropogenic SF effect, black line – panel (B), clearly follows the evolution of the aerosol direct effect which is much larger than the aerosol direct RF effect. The SF graph also shows that the anthropogenic, globally and annually averaged aerosol direct effect in 2000 at -1.6W/m^2 is comparable to the explosive volcanic eruptions of Krakatau (1883) -2.2W/m^2 and Pinatubo (1991) -1.8W/m^2 which are considered to affect the mid to high latitude atmospheric circulation patterns [*Solomon et al.*, 2007].

Absorbing aerosols, particularly black carbon, a product of incomplete combustion [*Novakov et al.*, 2003], and organic carbon [*Kirchstetter*, 2004], have been linked to variations in the vertical temperature profile of the atmosphere and the large scale atmospheric circulation [*Solomon et al.*, 2007], [*Menon et al.*, 2002] and [*Wang*, 2004]. Aerosols may also have a greater influence on the hydrologic cycle than other forcing agents through their SF effects [*Solomon et al.*, 2007].

Knippertz et al. [2015] discuss the effects of aerosols on the West African monsoon noting that "In West Africa, biomass burning is a large direct source of carbonaceous aerosols" and "Biomass burning occurs predominantly during the dry season. It is almost exclusively anthropogenic…". It is also noted that "more attention should be paid to rapidly increasing air pollution over the explosively growing cities of West Africa, as experiences from other regions suggest that this can alter regional climate through the influences of aerosols on clouds and radiation".

Solomon et al. [2007] expressed the concern that the distribution and evolution of aerosol emissions during the 20th century were not well understood and *Hegerl et al.* [2007] noted that most studies used in the IPCC AR4 omitted carbonaceous aerosols which could have significant effects at regional scales.

The effects of short lived gases and aerosols were found to be substantial compared to LLGHG and to account for as much as 40% of the warming over the summertime United States and the climate response to these forcing agents was not confined to the area of their emission [*Levy II et al.*, 2008].

The global aerosol coverage and forcing is highly variable geographically and temporally and it is "insufficient or even misleading" to emphasise the global average and the aerosol SF is greater than the RF at the top of the atmosphere. Such SF affects the atmospheric circulation and the hydrologic cycle [*Remer et al.*, 2009].

Menon et al. [2002] investigating the climate of China and India found precipitation and temperature changes in their model that were comparable to those observed only if the aerosol ensemble included a large proportion of absorbing black carbon ("soot") which was similar to observed amounts and noted that absorbing aerosols heat the atmosphere and alter the regional atmospheric stability and vertical motions which affects the large-scale circulation and hydrologic cycle with significant regional climate effects.

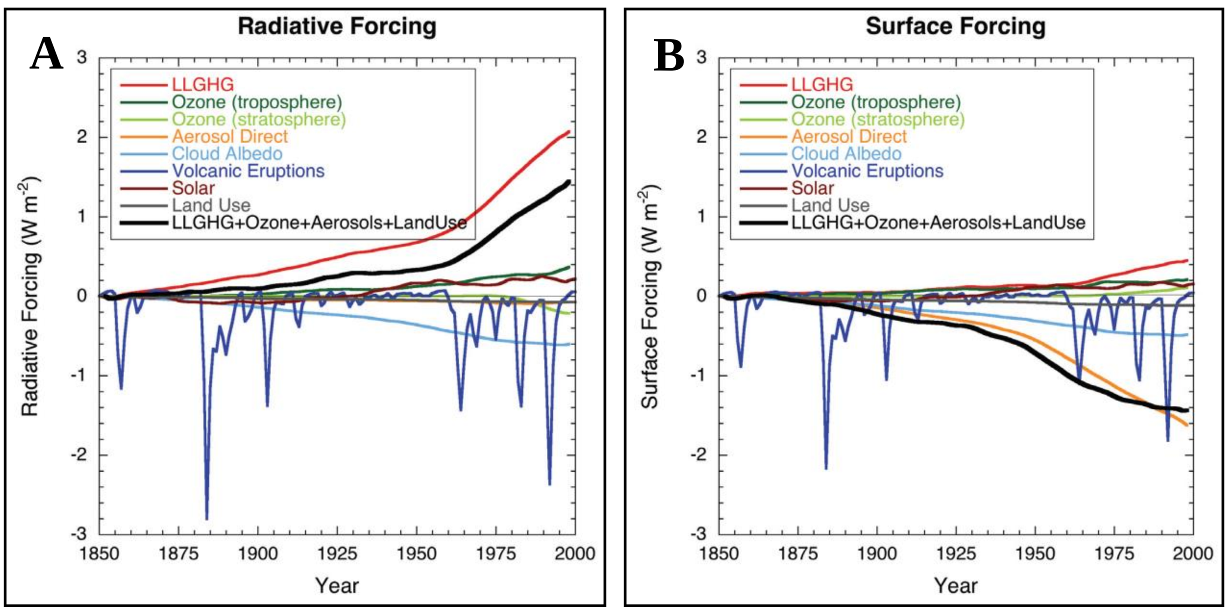

Figure 2: IPCC AR4 Figure 2.23 Chapter 2 page 208 [Forster et al., 2007]. Globally and annually averaged temporal evolution of the instantaneous all-sky RF (A) and SF (B) due to various agents, as simulated in the MIROC+SPRINTARS model (Nozawa et al., 2005; Takemura et al., 2005). This is an illustrative example of the forcings as implemented and computed in one of the climate models participating in the AR4. Note that there could be differences in the RFs among models. Most models simulate roughly similar evolution of the LLGHGs' RF.

Anthropogenic aerosols have been linked to: the decadal variance in the North Atlantic SST and thus to drought in the Sahel and the Amazon with the dominant mechanism being the reduction in short wave surface radiation [*Booth et al.*, 2012]; and the expansion of the tropics in the northern hemisphere evidenced by a poleward shift of the Hadley Cells, subtropical dry zones and extra-tropical storm tracks [*Allen et al.*, 2012] who identify West Africa as one of the regions of the globe which has demonstrated increases in black carbon emissions of 1ng/Kg from 1970 to 2009. However *Zhang et al.* [2013] investigated the claims in [*Booth et al.*, 2012] and concluded that "key aspects of the HadGEM2-ES simulation exhibit substantial discrepancies with observations." Whilst noting that

"Anthropogenic and natural aerosols have likely played some role in forcing the observed Atlantic mutidecadal variability."

[*Ott et al.*, 2010] investigated the extreme biomass burning episode in the south East Asia in 2006 and found that "temperatures over Indonesia were strongly modified by increased diabatic heating during the period of burning. The largest increases were found in October and November between 150 and 400 hPa. In some regions, increases exceeded 0.7 K during SON." and that it is necessary for GCMs to include realistic representations of aerosols which fully represent the interannual variability of biomass burning emissions in order to capture the effects discussed in their paper.

The carbonaceous aerosol emission inventories for the Coupled Model Intercomparison Project phase 5 (CMIP5) are based on *Lamarque et al.* [2010] and are decadal averages designed to investigate long term (decadal to century) climate change and *Lamarque et al.* [2010] specifically state the emission inventories for CMIP5 are not designed to investigate "rapid" (i.e. less than a few years) pollution changes which this paper addresses.

Booth et al. [2012] also note that future emissions of anthropogenic aerosols are "directly addressable by policy actions".

In summary then the literature states aerosols affect:

1. The hydrologic cycle;
2. The large-scale atmospheric circulation systems; and
3. are not well understood;

and that carbonaceous aerosols:

1. Are an essential parameter in climate models to correctly model observed changes in precipitation;
2. Were omitted from most studies used in the IPCC AR4;
3. Have recently been linked to significant climate events; and
4. Are only included in the CMIP 5 RCP's as decadal averages which cannot model the effects this paper addresses.

and that aerosol emissions are directly addressable by government policy actions.

The term Aerosol Regional Dimming (ARD) describes the surface radiative forcing effect of continental scale aerosol plumes which immediately alters the large-scale atmospheric circulation systems and regional hydrologic cycle and, crucially, only occurs when the plume exists.

1.7 The Anthropogenic West African Aerosol Plume

The major anthropogenic aerosol plume located in the region most likely to affect the European region Hadley Circulation occurs over West Africa and is referred to as the West African aerosol Plume (WAP).

The WAP is one of eight great aerosol plumes [*Potts*, 2017] which occur annually. It can be identified on the monthly mean 0.55 micron AOD data from MODIS [*Kaufman et al.*, 2000] on the NASA Terra and Aqua satellites distributed via the NASA MODIS Giovanni System (NMGS).

Remer et al. [2005] confirm that the uncertainty in the AOD measured by these two satellites is "$\Delta\tau=\pm 0.05 \pm 0.15\tau$ over land" and that the AOD retrievals can be used in monitoring the aerosol radiative forcing of the global climate. The area used to analyse the WAP is 0° to 10°N 0° to 10°E (WAP Area).

The monthly average AOD of the WAP Area and the annual AOD cycle are shown in Figures 3 and 4 to demonstrate the peak anthropogenic aerosol emission season is January, February and March (JFM), the end of the dry season in West Africa, and was extremely high in 2004, 2007, 2012, and 2016 compared with the intervening years. This paper therefore focuses on the anthropogenic WAP in JFM because it is at its most intense in this season and will therefore have its greatest effect at this time. Figure 4 shows the trend in AOD since 1980 using the MERRA-2 reanalysis data and Figure 5 shows the geographic extent of the JFM 2004 extreme apparition of the WAP and clearly shows the origin of the plume to be in southern Nigeria as the highest AOD levels are seen there.

The maximum AOD for the WAP Area measured by the MODIS sensor on the Terra platform was 1.32 (Mar 2004) and the trend line of the MERRA-2 AOD in JFM in the WAP Area increased from 0.5 in 1980 to 0.76 in 2019 a 52% increase. From 1980 to 2004, a major biomass burning event year, the increase in AOD in March was from 0.37 to 1.10 an increase of 197%.

Oluleye et al. [2012] investigated the relationship between the AOD retrievals from the NASA Terra and Aqua satellites and ground-based photometers in West Africa and found good correlations, over 0.90, at Ilorin in Nigeria. Figure 2 in that reports clearly shows the seasonal variation in the AOD levels with many days showing AOD levels at Ilorin over 1.00 in JFM from 2005 to 2009.

WAP History: Figure 4 shows a significant trend in the AOD of the WAP from 1980 to 2019 and the WAP AOD would have been significantly lower in 1950 than it was in 1980 for two reasons:

- First: the population of West Africa was significantly higher in 1980 (188 million) c.f. 1950 (71 million) (United Nations World population data for West Africa) which implies less biomass burning from agriculture and land clearing; and
- Second: oil production had not started in Nigeria in 1950 (Nigerian National Petroleum Corporation in "History of the Nigerian Petroleum Industry" at https://www.nnpcgroup.com/NNPC-Business/Business-Information/Pages/Industry-History.aspx and there were therefore no gas flares driven by oil production in Nigeria in 1950.

This suggests that the AOD of the WAP in JFM in 1950 would have been beneath 0.19 on the basis of pro rata population growth alone and perhaps beneath 0.1 without the gas flares. This implies the effects of the extreme WAP are very recent and that the anthropogenic WAP did not exist in its present extreme state in JFM prior to or in the early 1950's.

The main sources of aerosols in the WAP are described in detail in Appendix A.

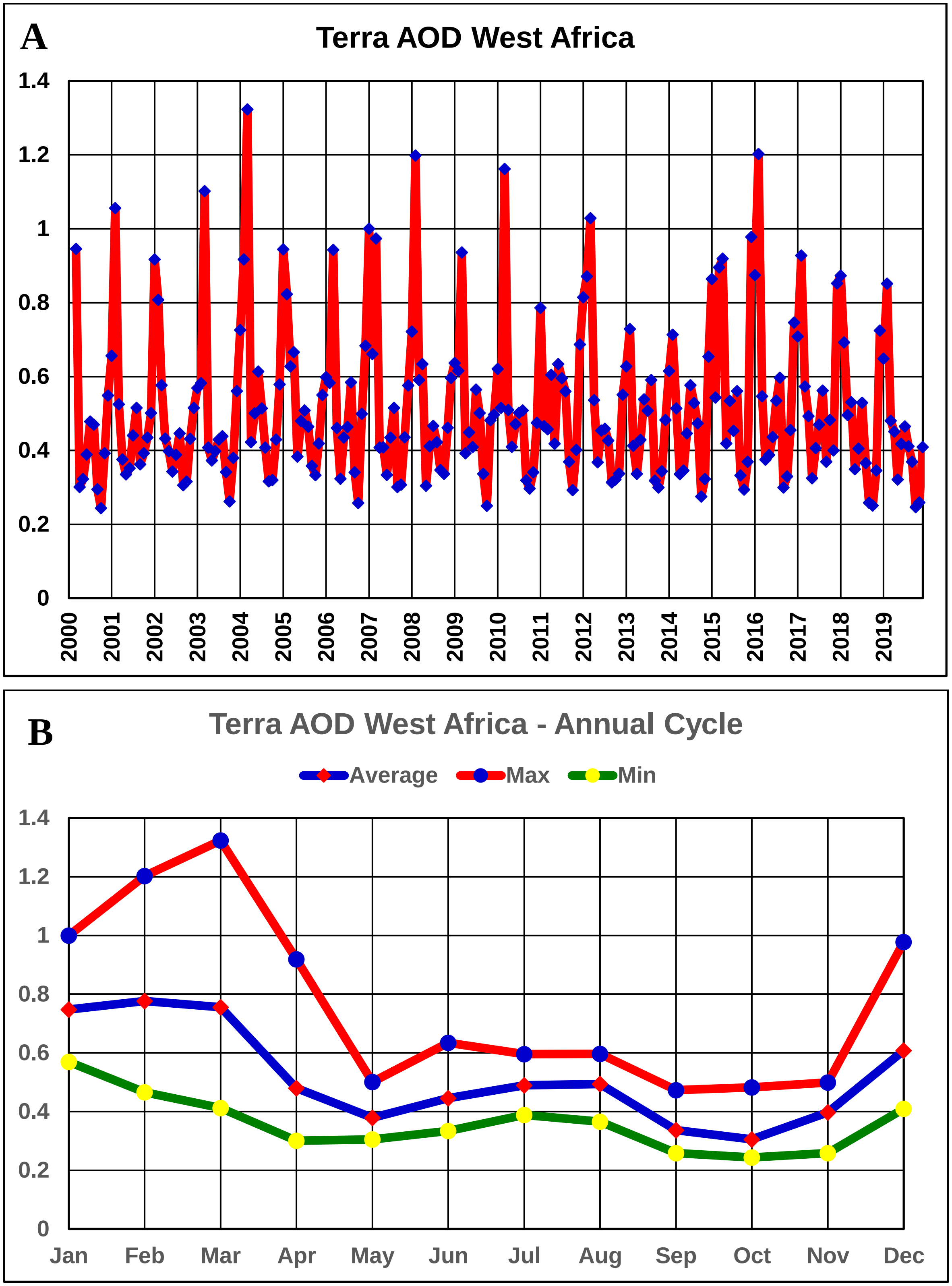

Figure 3: Terra Monthly AOD WAP Area. A; Average, Max and Min Annual cycle B.

.

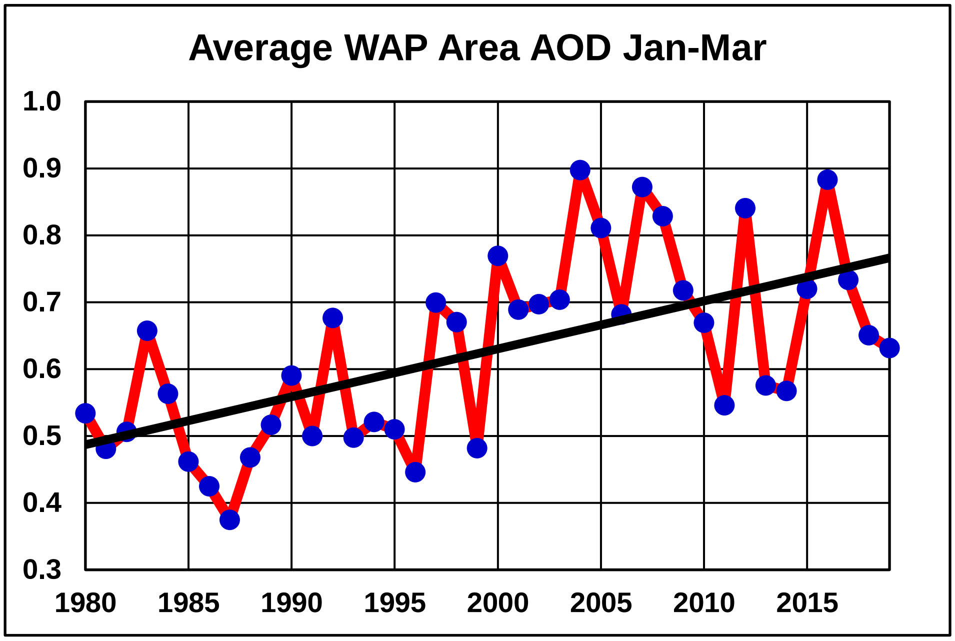

Figure 4: Average MERRA-2 JFM AOD WAP Area.

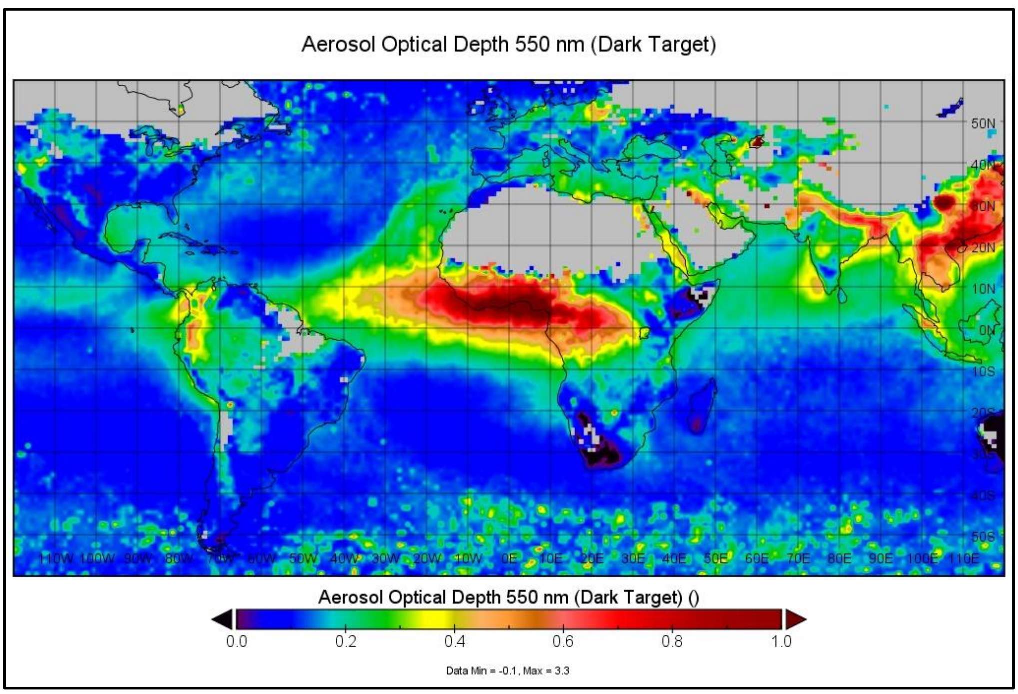

Figure 5: NASA Terra average AOD Jan - March 2004.

1.8 Surface Radiative Forcing by Aerosols

The SF of aerosols is significant and the literature includes:

1. a 10% to 30% reduction of Photosynthetically Active Radiation recorded during INDOEX in the Indian Ocean in 1999 [Ramanathan, 2006];
2. $-150\ \mathrm{W\ m^{-2}}$ in an analysis of the Indonesian wildfires which occurred in 1997 in [Duncan et al., 2003]; and
3. $\sim -286.0(\mathrm{W/\ m^2})/\tau\alpha$ recorded during the Aerosol Characterization Experiment -Asia in 2001 [Hansell et al., 2003] ($\tau\alpha$ is the aerosol optical depth and its derivation is described in the paper).

The idealised change in direct surface radiation when the WAP is present is shown in Figure 6 with a plume AOD estimated at 0.8 compared with background 0.58 giving an estimated 20% reduction in surface radiation noting that 0.8 is less than the maxima shown in the MERRA-2 data in Figure 4 and 0.58 is greater than lower minima in the same Figure which implies the actual reduction in surface radiation may be greater than 20%. In Figure 6 the sun is assumed to be over the equator and the phase lag between the sun and the position of the ITCZ is ignored. It is clear that the highest level of surface solar radiation is at the edges of the plume and that these regions will drive convection which, in turn, drive the Hadley Cells. With the convective drive of the regional northern Hadley Cell moving north the entire northern regional Hadley Cell is perturbed which in turn perturbs the regional sub-tropical ridge in the northern hemisphere and creates anomalous, persistent, high pressure over the Mediterranean, Iberia and the Eastern Atlantic (MIEA) as a direct consequence of the WAP.

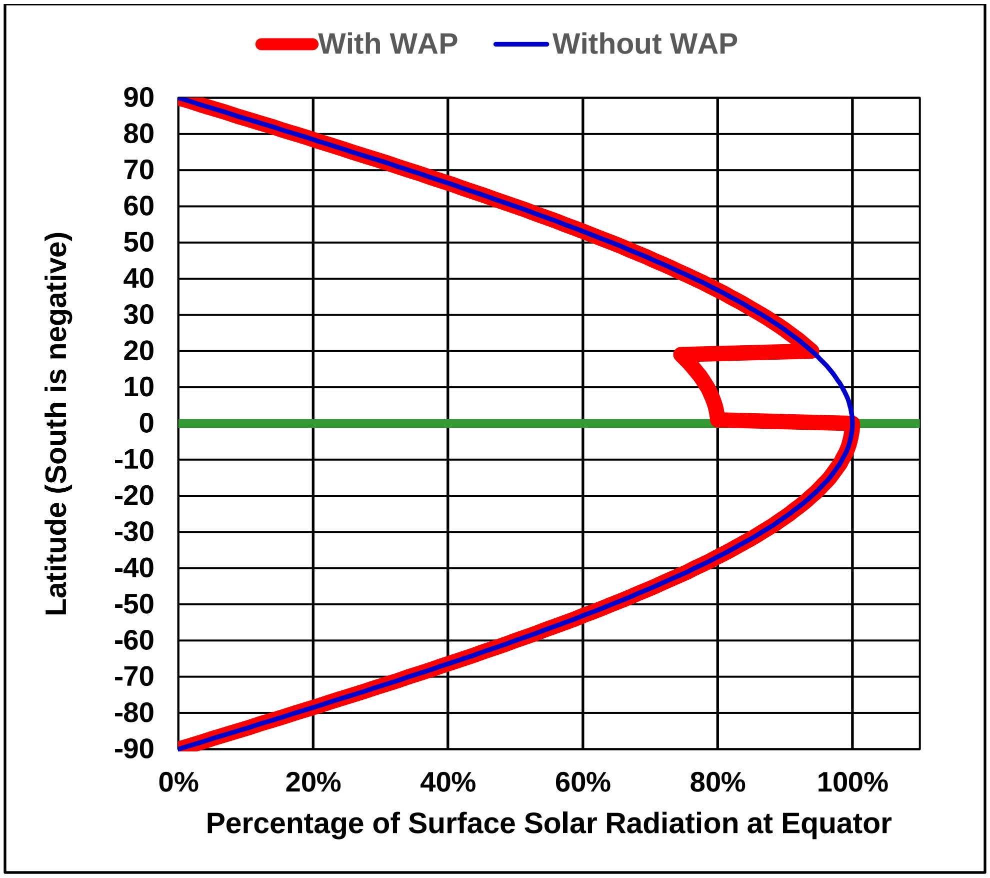

Figure 6: Idealised surface solar radiation with and without the WAP assuming a reduction surface radiation of 20% and a 20° latitude width of the WAP from 0° to 20°N.

2 METHOD and DATA

2.1 Modelling Data

The Last Millennium Ensemble (LME) [*Otto-Bliesner et al.*, 2016] data is available at https://www.earthsystemgrid.org/ . One member of each of the eight LME forcing simulations with run number in () (850 (3), All (13), Ozone and Aerosol (Aero) (2), Green House Gas (GHG) (3), Land use (Land) (3), Orbital (3), Solar (5) and Volcanic (5)) was used to create time series of 1,156 years of: AODVIS (hereinafter AOD); surface pressure (PSL), surface temperature (TS); precipitation (PRECL) and vertical pressure velocity (hereinafter "omega"); The LME data was averaged to give annual and JFM time series from 850 to 2005 and then correlated with the WAP AOD as a time series to demonstrate that these indices and parameters are directly connected to aerosols in the WAP area.

The data was also segmented and averaged on the basis of AOD and then correlated and is also presented graphically to show the effects of changes in AOD without using correlation.

Areas used for the LME data (Descriptors in ()) are shown in Figure 7 and are:

- AOD (WAP Area): 0° 10°N and 0° 10°E

- Surface Temperature (WAP Area) 0° 10°N and 0° 10°E
- Omega West Africa (W. Africa) 10° 15°N and 0° 10E°
- Pressure (Mediterranean, Iberia, Eastern Atlantic (MIEA)): 30° 45°N and 30°W 15°E
- Rainfall Southern Europe (Iberia): 35° 43°N and 20°W 10°E
- Rainfall Northern Europe (UK/Ireland): 50° 60°N and 10°W 10°E
- Temperature (N. Europe): 45° 60°N and 15°W 30°E

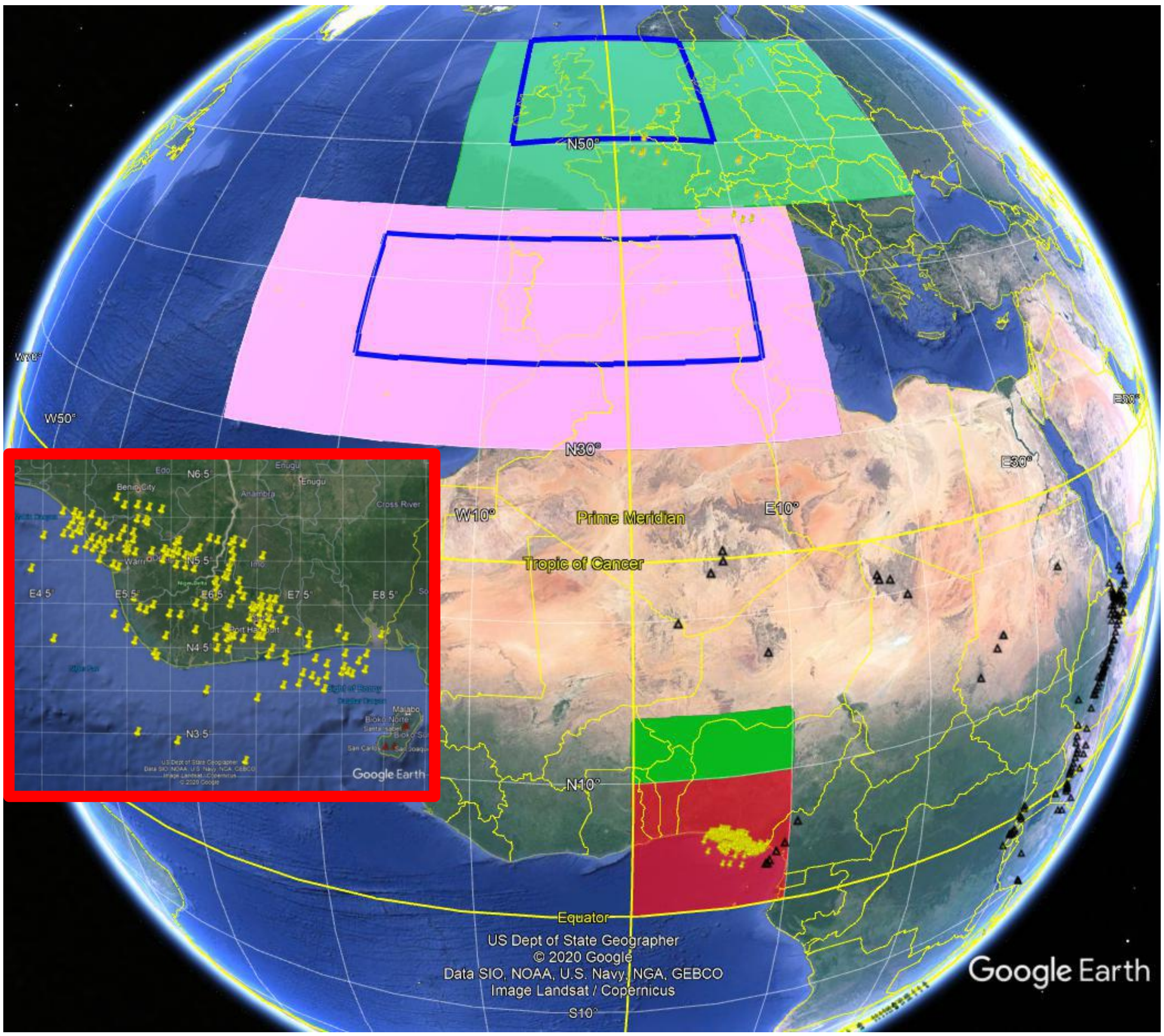

Figure 7: Google Earth image showing areas used and the locations of Nigerian gas flares (National Oceanic and Atmospheric Administration (NOAA) and the Global Gas Flaring Reduction Partnership (GGFRP)) in yellow and African volcanoes (Global Volcanism Program) in black. Inset southern Nigerian gas flares.

2.2 MERRA-2 Data

A similar approach was used for the NASA Modern Era Retrospective analysis for Research and Applications release two (MERRA-2) reanalysis dataset [*Gelaro et al.*, 2017] which is an atmospheric reanalysis of the modern satellite era produced by NASA's Global Modelling and Assimilation Office. MERRA-2 is especially useful for the analysis in this paper as it includes the assimilation of aerosol observations and extended for 40 years in 2019. The aerosol loading in the WAP area is variable with significant spikes at near random intervals making it especially useful in correlation analysis. Data http://giovanni.gsfc.nasa.gov/giovanni/

3 RESULTS

The climate is highly variable with more than one agent usually contributing to any variation and therefore whilst useful information can be extracted from such data using only time series analysis it is preferable to also analyse the data by segmenting the data on the basis of the forcing agent being investigated, averaging and then correlating as the averaging process improves the signal to noise ratio in the data significantly and the range of the forced parameter from the lowest to the highest forcing segment shows the effects of the forcing agent without relying on correlation.

The LME time series correlations are presented in Figure 8 where the time series annual data shows lower correlation magnitudes than the JFM data. This results from the "smearing" of the extreme plume across the entire year and is only included to demonstrate that aerosols must be modelled at spatial and temporal resolutions which can correctly model the plume. The focus of this paper is on the JFM data when the anthropogenic WAP is at the most extreme levels.

It is worth noting that the range of AOD in the three datasets used in JFM is Terra 0.6 to 1.1, MERRA-2 0.4 to 0.9 and the LME 0.3 to 1.1. The LME and MERRA-2 AOD ranges are similar whilst the Terra dataset (2000 to 2019) shows a higher low value than the others as the WAP was well established for the entire Terra dataset and was not for the LME and MERRA-2 data as Figure 4 shows.

Some of the correlations from the LME data show significance levels that are much less than 0.01 due to the correlation magnitude and the length of the time series.

Segment analysis results in the extraordinary correlations shown in the last two rows of Figure 8 where the majority are 0.99 magnitude and these results are then discussed sequentially following the hypothesis and physical model.

Figure 9 shows the MERRA-2 JFM segmented data analysis.

The comparison data in the sections below is created by subtracting the 1987 data from the 2004 data using either the MERRA-2 data via NASA Panoply or the NCEP/NCAR reanalysis data which is sourced from the NCEP/NCAR website at https://www.esrl.noaa.gov/psd/cgi-bin/data/composites/printpage.pl .

AOD	Omega (609mb)	Surface Temp. WAP Area	Surface Pressure	Precipitation S. Europe	Precipitation UK/Ireland	Temperature N. Europe
Time Series						
Annual	0.21	-0.41	0.71	-0.63	0.26	0.30
JFM	0.72	-0.60	0.75	-0.64	0.41	0.45
Segmented						
Annual	0.96	-0.97	0.99	-0.99	0.97	0.99
JFM	0.99	-0.99	0.99	-0.99	0.97	0.98

Figure 8 LME correlations of AOD in the WAP Area with the parameters shown. Note: Colour coding for the correlation significance in all results is Green <0.05 and Yellow < 0.01.

AOD	Omega (825hPa)	Surface Temp. WAP Area	Surface Pressure	Precipitation S. Europe	Precipitation UK/Ireland	Temperature N. Europe
Segmented						
JFM	0.95	-0.98	0.99	-0.99	0.92	0.98

Figure 9 MERRA-2 correlations of AOD in the WAP Area with the parameters shown

3.1 The WAP Forms

Area used: 0° 10°N and 0° 10°E

The intense WAP forms in late December and disperses in April as Figure 3 shows. Figure 10 shows the extreme WAP in JFM in 2004 compared to the 1987 apparition with a significant increase in AOD of over 0.6 across much of the WAP Area.

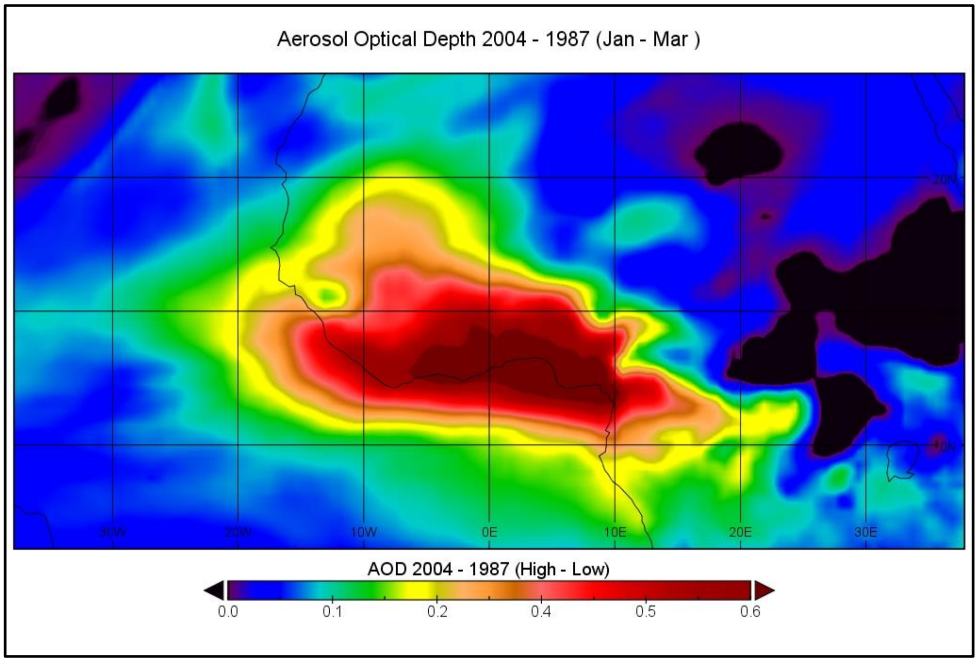

Figure 10: MERRA-2 AOD JFM 2004-1987

3.2 The WAP absorbs Solar Radiation and Heats the Atmosphere

Area used: **2**0°S to 40°N and 0° to 10°E

Change: Figure 11 shows the MERRA-2 air temperature averaged across the WAP Area longitudes from 20°S to 40°N and it can be clearly seen that in the high AOD year the air temperature within the plume at 700hPa to 850hPa is higher which correlates reasonably well with estimated aerosol height from the CALIPSO data [*Winker et al.*, 2009] which on 1 January 2016 (a high AOD year in the WAP Area) showed elevated aerosols at altitudes from 1.0 to 5.0 km.

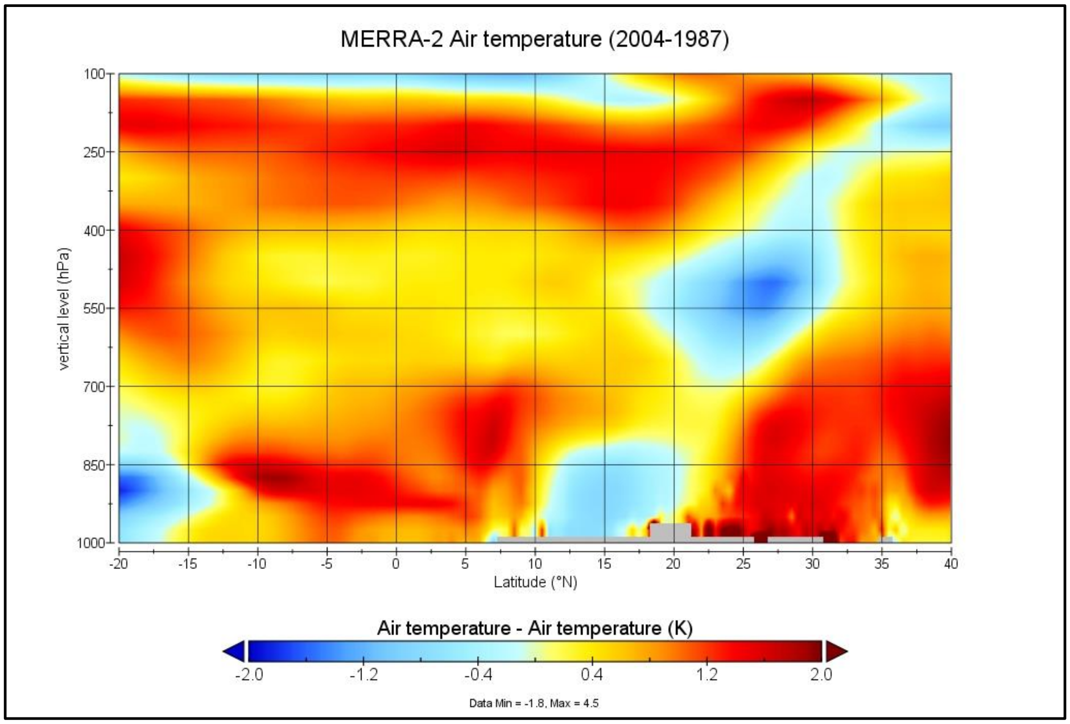

Figure 11: MERRA-2 JFM Air Temperature averaged across the WAP Area Longitudes 2004-1987

3.3 The WAP Reduces the WAP Area Surface Temperature

Area used: 0° 10°N and 0° 10°E

Correlation: -0.99 with r^2 values 0.97 leaving no room for other significant influences.

Change: Figure 12 shows a reduction of 1.2° K in the JFM surface temperature from the segment with the lowest AOD to the highest and Figure 13 shows the change in West Africa in JFM between 2004 and 1987 with parts of the WAP Area cooling by over 2° K.

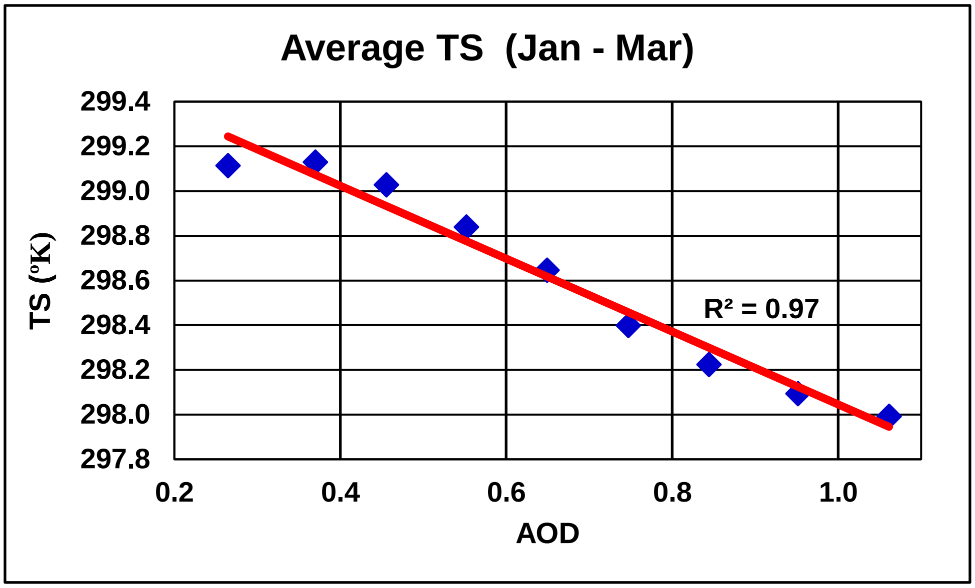

Figure 12: LME JFM Surface Temperature and WAP Area AOD. Segmented and averaged.

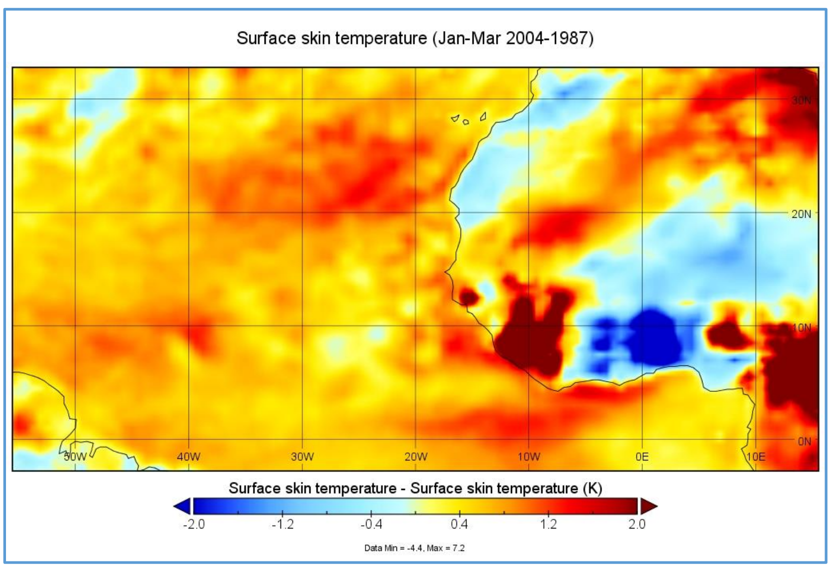

Figure 13: MERRA-2 Surface Skin Temperature (TS) Jan-Mar 2004 – 1987.

3.4 The WAP Reduces Convection in West Africa

Area used: 10° 15°N and 0° 10E°

Correlation: 0.99 with r^2 values 0.98 leaving no room for other significant influences.

Change: Figure 14 shows an increase in JFM omega from -0.16 to 0.10 from the lowest AOD to the highest implying a reduction in convection with the higher AOD levels having a positive value of omega indicating that the normal convection with low AOD in West Africa has, in fact, reversed.

Note: omega is pressure velocity and rising air therefore has a negative velocity as it is moving from higher to lower pressure. A reduction in convection is therefore a positive change in omega and as aerosols reduce convection in the WAP Area the correlations of omega and AOD are positive.

In Figure 14 the annual data has been included to demonstrate how averaging the effects of aerosol plumes annually when the plume only exists for a few months completely destroys the significant effects of the plume when it exists. The annually averaged data shows omega only rises from -0.017 to -0.015 and the reversal of convection seen in the JFM data is masked by the averaging process.

The effects of carbonaceous aerosols on convection and atmospheric circulation have been extensively described in the literature as discussed in the introduction. The WAP absorbs solar radiation which warms the upper atmosphere and reduces solar radiation at the surface which cools the lower atmosphere. This alters the vertical temperature profile of the atmosphere with warmer air above cooler air (relative to the temperatures without the plume) and this stabilises the atmosphere and reduces convection. This well understood process is confirmed in the WAP Area in this paper with the demonstrated correlation of omega with the AOD and in Figure 14.

The WAP also moves the northern Hadley Cell convection column in West Africa north as Figure 15 shows where omega increases over land in West Africa where the plume exists and from 35 to 45 north where the anomalous high pressure over the MIEA exists.

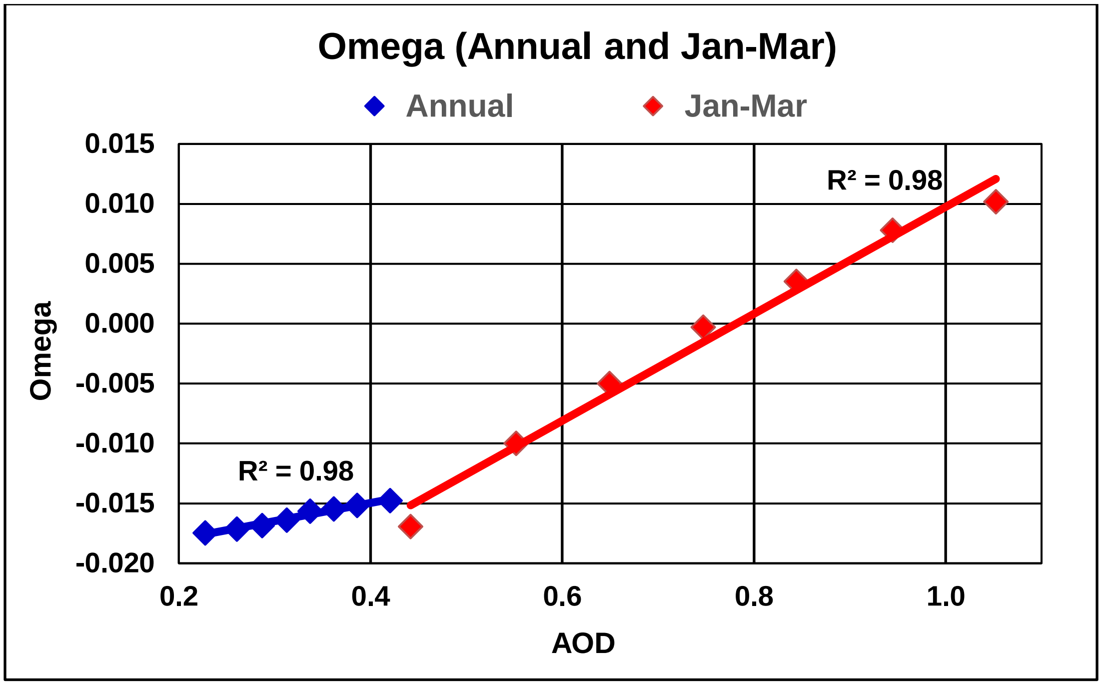

Figure 14: LME Annual and JFM Omega and WAP Area AOD segmented and averaged

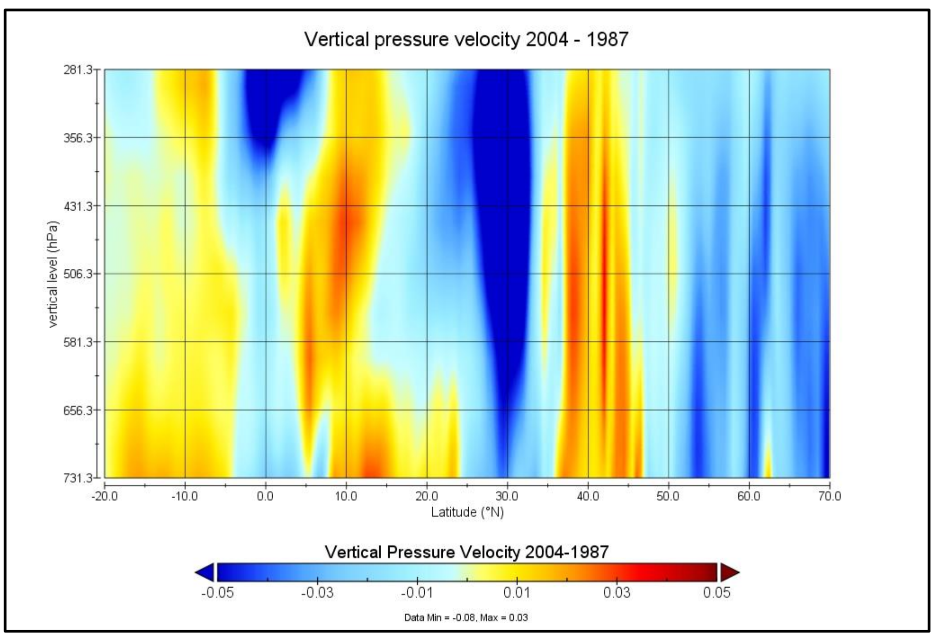

Figure 15: MERRA-2 JFM Omega 2004-1987.

3.5 The WAP Perturbs the Hadley Circulation:

The Hadley Cells are thermally driven [*McGregor and Nieuwolf*, 1977], [*Barry and Chorley*, 2010] and [*IPCC*, 2007]. Reduced convection in the WAP Area alters the regional Hadley Cells and this can be clearly seen in Figure 15 where the rising limb of the northern Hadley Cell has been altered in the year of high AOD in the WAP Area relative to the low AOD year and the region driving the greatest increase in convection is between 25° and 35° north.

3.6 The Crucial Step – The WAP Increases Surface Pressure in the MIEA

Area used: 30° 45°N and 30°W 15°E

Correlation: 0.99 with r^2 values 0.99 leaving no room for other significant influences.

Change: Figure 15 shows the vertical profile of omega from 20S to 70N across the WAP Area longitudes and it is clear that a major change in omega occurs between 35N and 45N where an increase in omega in the high WAP AOD years leads to the higher pressure over the MIEA.

Figure 16 shows surface pressure rises from 1018.0 to 1026.9 hPa from the segment with the lowest AOD to the segment with the highest a rise of 8.9 hPa which is comparable to the observed increase shown in Figure 7 in [*van Oldenborgh et al.*, 2009].

Figure 17 shows the difference between 2004 and 1987

Note: This is the crucial step in the changes induced by the WAP and it is the only change remote from West Africa directly forced by the WAP with all other changes, drought in Iberia, flooding in the UK/Ireland and higher winter temperatures in northern Europe driven by this anomalous region of increased surface pressure.

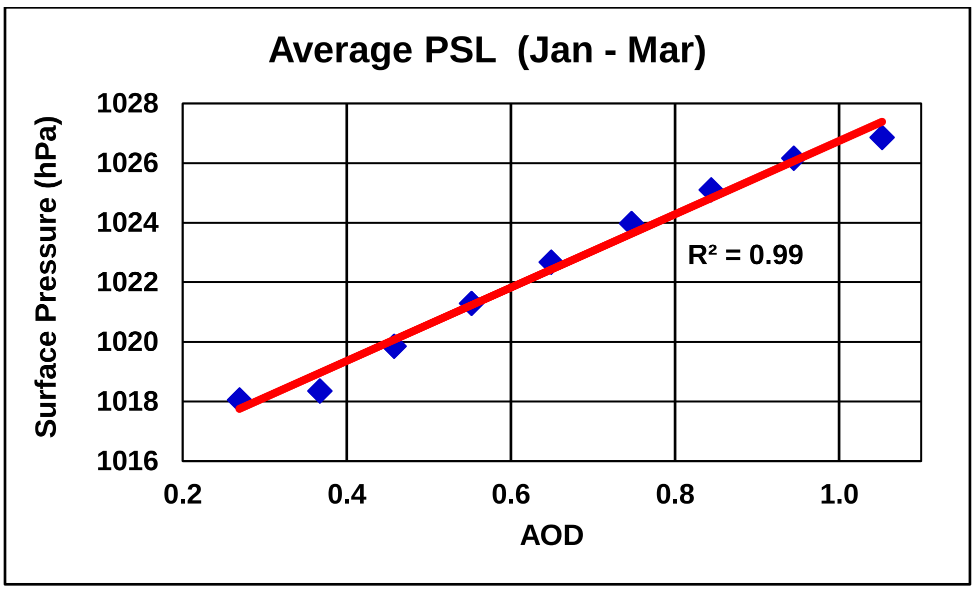

Figure 16: LME JFM Surface Pressure and WAP Area AOD. Segmented and averaged.

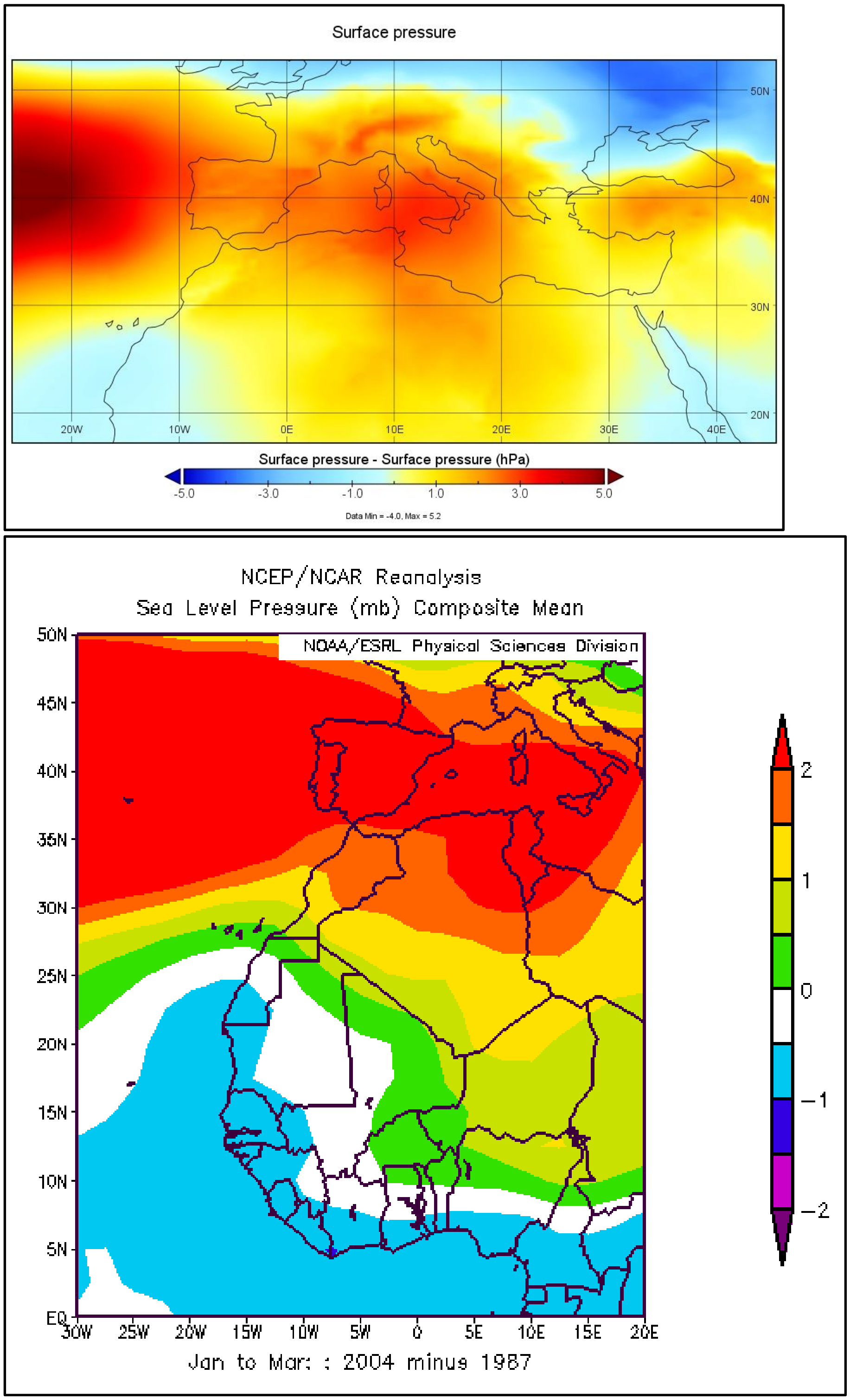

Figure 17: MERRA-2 and NCEP/NCAR Surface Pressure change 2004-1987

3.7 The WAP Reduces Precipitation in Iberia

Area used: 35° 43°N and 20°W 10°E

Correlation: -0.99 with r^2 values 0.99 leaving no room for other significant influences.

Change: Figure 18 shows precipitation falls from 191mm to 60 mm from the segment with the lowest AOD to the segment with the highest, a fall of 131 mm or 69% and Figure 19 shows the difference between 2004 and 1987 where most of the MIEA shows a reduction in rainfall of over 8mm/month.

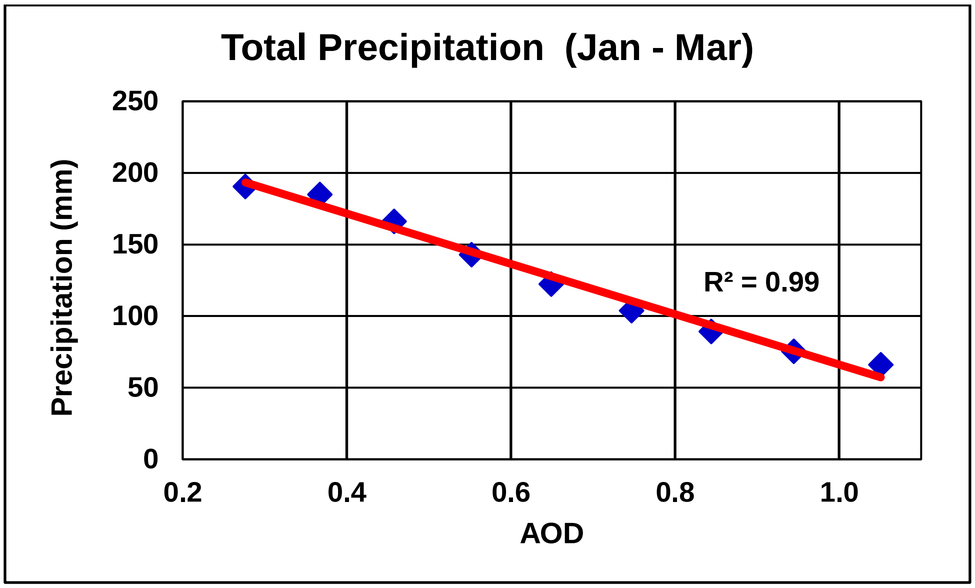

Figure 18: LME JFM MIEA Precipitation and WAP Area AOD. Segmented and Averaged.

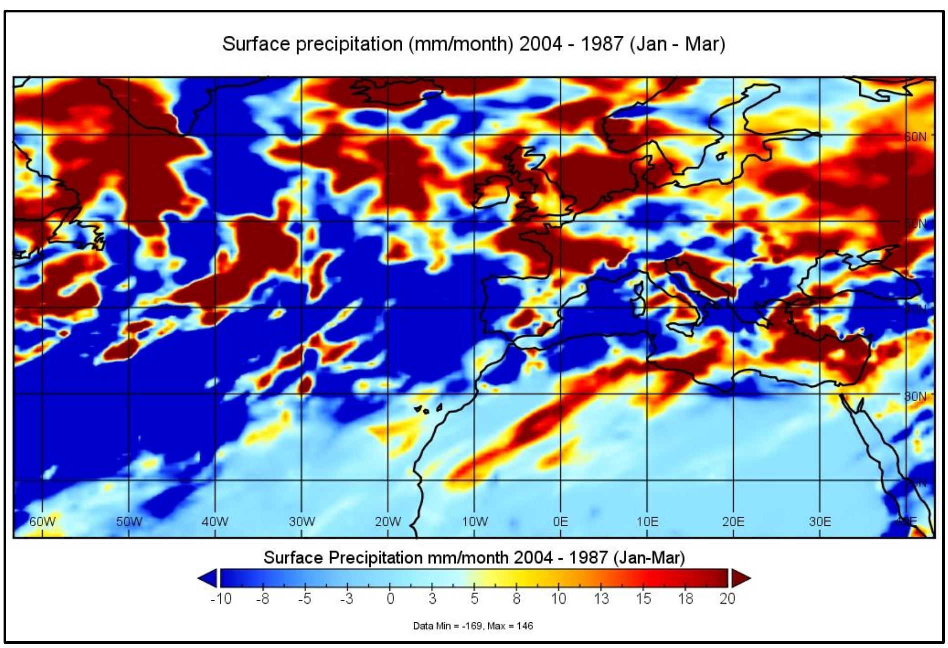

Figure 19: MERRA-2 JFM Precipitation 2004-1987

3.8 The WAP Advects Warm, Moist Air into Northern Europe

With high pressure established over the MIEA, as Figure 17 shows the natural wind flows are significantly perturbed as Figure 20 shows. A strong flow is visible from the Atlantic Ocean east of the USA across the Atlantic and into the UK/Ireland and northern Europe. This probably constitutes yet another atmospheric river, see *Ralph and Dettinger* [2011] for an early overview, [*Lavers and Villarini*, 2013] and [*Young et al.*, 2017], carrying significant moisture from the warm ocean to the UK/Ireland and northern Europe.

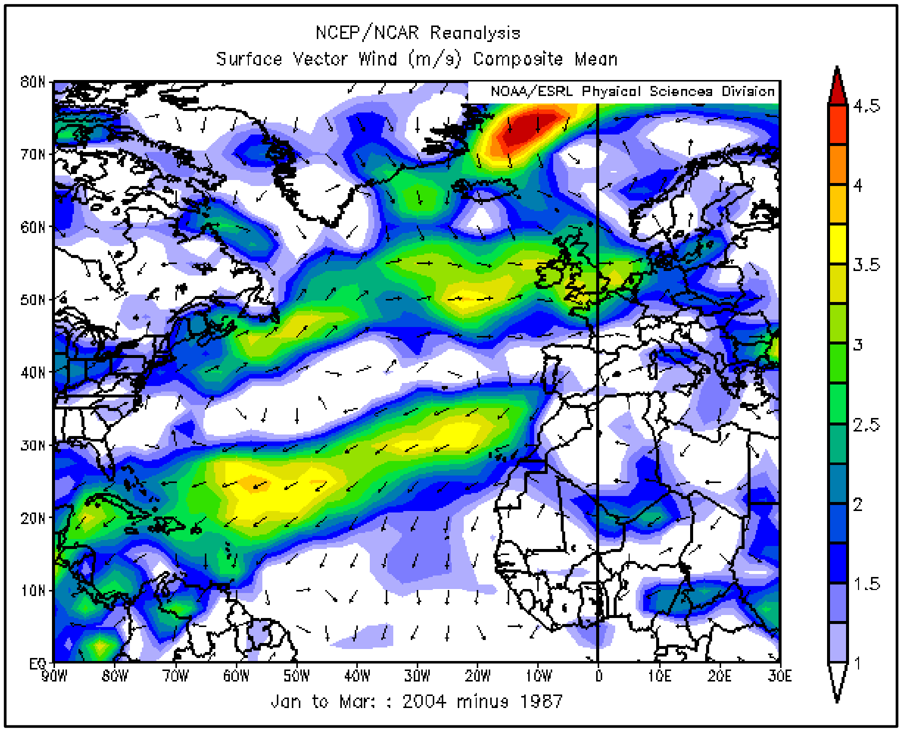

Figure 20: NCEP/NCAR JFM Surface Vector Wind 2004-1987

3.9 The WAP Increases Precipitation in the UK and Ireland

Area used: 50° 60°N and 10°W 10°E

Correlation: 0.97 with r^2 values 0.94 leaving no room for other significant influences.

Change: Figure 21 shows precipitation rises from 382 mm to 582 mm from the segment with the lowest AOD to the segment with the highest a rise of 200 mm or 52% and Figure 19 shows the difference between 2004 and 1987 with the west of England, Scotland and Northern Ireland receiving an increase in rainfall of over 20mm/month.

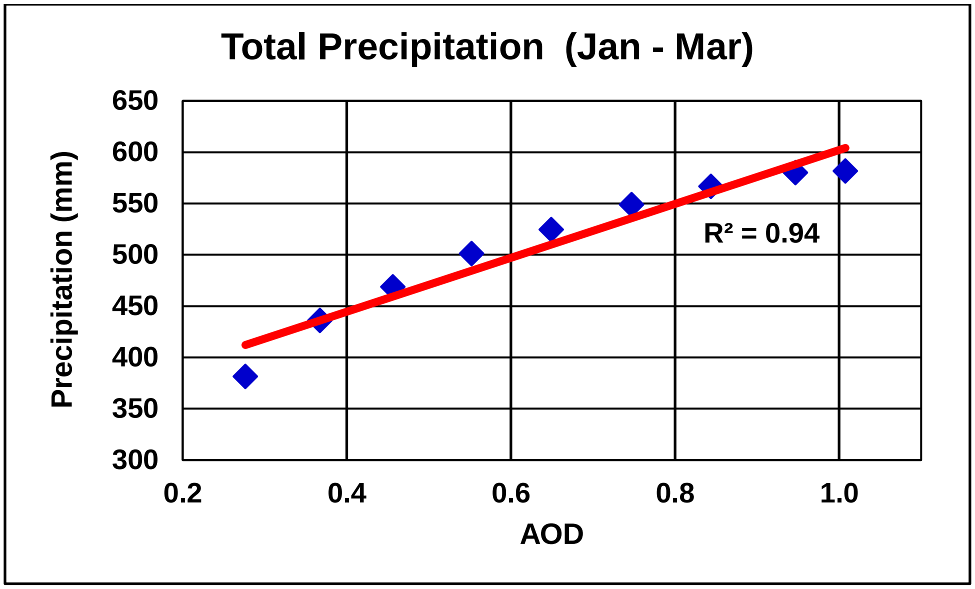

Figure 21: LME JFM UK/Ireland Precipitation and WAP Area AOD. Segmented and averaged.

3.10 The WAP Increases the Temperature in Northern Europe

Area Used: 45° 60°N and 15°W 30°E

Correlation: 0.98 with r^2 values 0.96 leaving no room for other significant influences.

Change: Figure 22 shows the temperature in northern Europe rises from 277.7° K to 279.6° K from the segment with the lowest AOD to the segment with the highest a rise of 1.9 ° K. and Figure 23 shows the difference between 2004 and 1987 where significant parts of Europe north of the Alps including Scandinavia show rises of over 4° K in the year of high WAP Area AOD.

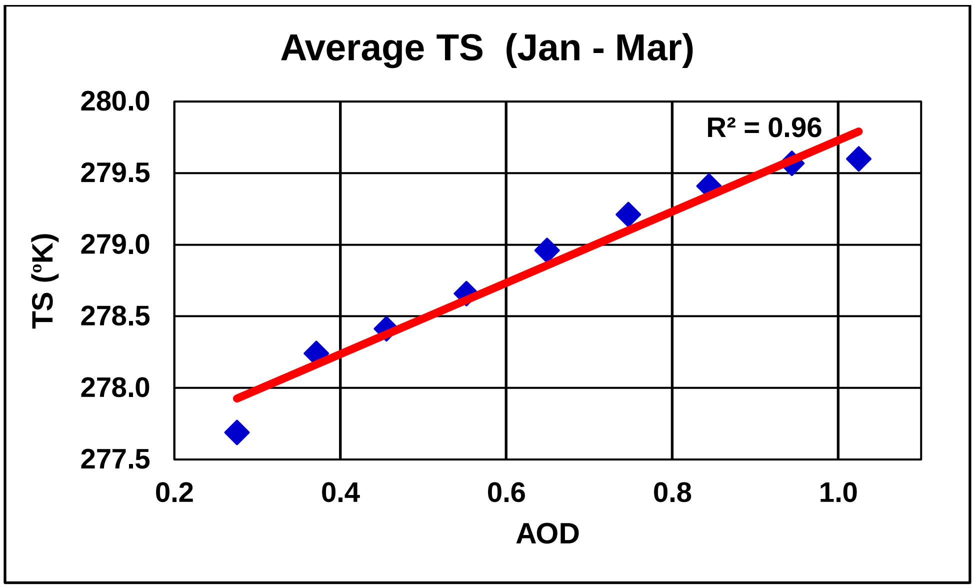

Figure 22: LME JFM Northern European Temperatures and WAP Area AOD. Segmented and averaged

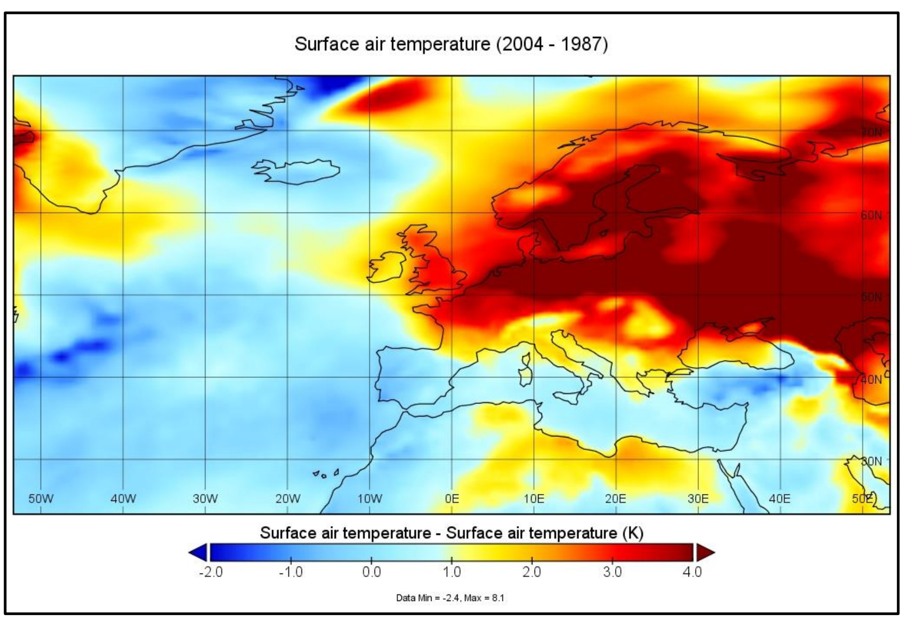

Figure 23: MERRRA-2 Surface Temperature 2004 - 1987

4 CAUSATION ANALYSIS

It is clearly understood that correlation between events A and B does not prove causation from A to B or vice versa. Thus, the causal relationship between the WAP and the European climate must be demonstrated in other ways.

4.1 Analysis without Correlation

Figure 18 shows that the LME JFM precipitation in Iberia falls from 191 mm to 60 mm a fall of 69% from the segment with the lowest AOD to the one with the highest and this is comparable to the fall in the measured Iberian rainfall in the 2004/05 water year of -60% [*García-Herrera et al.*, 2007]without using correlation.

4.2 Modelling

LME: there is no physical mechanism by which drought or SLP in Iberia can create aerosols in the LME over West Africa hence the causal direction must run from the aerosols to the rainfall and SLP.

In addition, the aerosol forcings in all LME runs are fixed at 1850 values except for the "ozone and aerosol" and "all" runs and there can therefore be no forcing of the aerosols by any agent within these six runs and the causal direction must flow from the aerosols to the rainfall and SLP.

MERRA-2 reanalysis assimilates measured aerosol data and therefore the causal direction must be from the aerosols to the rainfall and SLP as it cannot be the reverse.

4.3 Multiple Independent Datasets

The eight LME modelling runs and the MERRA-2 reanalysis exhibit very low or negative correlations between the WAP AOD in the individual runs as shown in the correlation matrix in Appendix B with an overall average 0.0016. Hence the datasets are independent.

All the eight segmented LME and the MERRA-2 datasets show correlations at magnitude 0.98 or greater with the Iberian rainfall and MIEA SLP at significance of <0.01 or less and the chance that all these nine independent datasets show the same result and are wrong is the product of the significance i.e. 0.01^{-9} or 10^{-18}, a vanishingly small number.

4.4 Segmented Data

The climate is a chaotic system and my preferred way to analyse climate data is to segment, average the data as the averaging process will improve the signal to noise ratio of the analysis. When the LME WAP JFM AOD and rainfall and SLP data in Iberia and the MIEA is segmented on the basis of the AOD data and then averaged and correlated R^2 values of 0.99 (Figure 16 and 18) are found. This demonstrates clearly that the WAP is the major and possibly the only driver of reduced winter rainfall and increased SLP in Iberia and the MIEA.

The difference between the lowest LME WAP Area AOD segment and the highest shows a reduction in JFM precipitation in Iberia of 131 mm or 69% in Figure 18 with an obvious, well-established trend. Similarly, Figure 16 shows and increase in SLP of 8.9 hPa also with a well-established trend.

This analysis does not depend on correlation.

4.5 Another Event “C”

One possible explanation for the correlations shown in this paper is that another unknown event “C” causes the WAP all the other effects discussed in this paper simultaneously.

However, Appendix A shows the JFM WAP is unquestionably anthropogenic and caused by biomass burning in deliberately lit fires in West Africa and it is therefore impossible for another event to cause the WAP and this possibility must be rejected.

4.6 Causal Direction

Therefore with:

1. The segmented LME data showing an increase in pressure in the MIEA as the AOD level of the WAP rises without using correlation
2. The segmented LME data showing a reduction in rainfall in Iberia as the AOD level of the WAP rises without using correlation;
3. The segmented LME data showing an increase in rainfall in the UK/Ireland as the AOD level of the WAP rises without using correlation;
4. The segmented LME data showing an increase in temperature in northern Europe as the AOD level of the WAP rises without using correlation;
5. The LME time series analysis showing the same results across multiple independent datasets with a vanishingly small chance of error;
6. The LME data showing, by a preferred analysis method, extremely high correlations of AOD with surface pressure, precipitation and temperature which leave no possibility of other significant drivers;
7. The MERRA-2 data confirming the LME data;

the inevitable conclusion is that the hypothesis is proven and the WAP is the primary driver in JFM of increased: pressure over the MIEA; rainfall in the UK/Ireland; and temperature in northern Europe and reduced rainfall in Iberia and, based on r^2 values, is the sole driver.

5 FUTURE RESEARCH

5.1 Confirming the conclusions

To finally confirm the findings above I suggest that a further LME style analysis is undertaken in which an aerosol plume is created in the model which ramps up from the naturally low level which existed in 1950 in December to reach the same AOD and geographic extent as the extreme JFM WAP of 2004 in January, continues at the same level to March and ramps down in April to the naturally low level which existed in May 1950. This plume to be applied in the model with random returns from 3 to 10 years to mimic the return frequency of high AOD events in Figure 4 with all other forcing agents held constant.

This modelling should be repeated with AOD levels reduced by perhaps 50% between runs to determine the level of AOD in the WAP Area which is required to create the effects demonstrated in this paper.

These experiments will confirm the analysis in this paper and provide the information governments will require to undertake the actions needed to reduce the WAP AOD to levels which will not impact the winter climate of Europe and will allow it to return to its natural state without the anthropogenic influence of the WAP.

5.2 Mitigating the WAP

5.2.1 Seasonal Biomass Burning

The most significant source of aerosols in the WAP is biomass burning which takes place towards the end of the dry season in West Africa in JFM. The biomass is burned for the reasons outlined in the Appendix.

Reducing the incidence of biomass burning requires the deployment of new technologies which are now available to take the unwanted biomass and convert it into useful products such as liquid fuel which, of course, would be carbon dioxide neutral as the feedstock is not a fossil fuel. MIT in 2015 produced a report into this technology: Biomass to Liquid Fuels Pathways [Seifkar et al., 2015] and there are many others such as [*Graham et al.*, 2011].

Deployment of this technology would enable the rapid reduction of in the AOD levels over West Africa as the technology would create a new income stream for farmers and others selling into a new industry and it would enable West African governments to ban biomass burning in the open as other governments have done.

5.2.2 Gas Flares

The anthropogenic WAP also comprises carbonaceous aerosols from the routine flaring of associated gas in the oil production industry. (Associated gas is gas dissolved in liquid oil which boils out of the liquid when the oil is produced from deep in the Earth (typically 1,500 to 3,000 metres depth) and the pressure reduces to atmospheric levels. Associated gas produced in areas without infrastructure to use the gas is flared. A process which is, indubitably, wasteful.)

The World Bank via the GGFRP has been trying to reduce routine flaring in the oil industry with some success in West Africa with the amount of gas flared in Nigeria reducing from 8.4 to 7.4 billion cubic metres (bcm) between 2014 and 2018 according the GGFRP website at https://www.worldbank.org/en/programs/gasflaringreduction#7 .

Even with this success the oil industry still flares a significant amount of gas in Nigeria which in 2018 was the 7th largest flaring country in the World and the industry should be required to immediately eliminate the routine flaring of gas by government or, at a minimum, flare the gas without creating aerosols.

5.2.3 Background AOD Levels

The background AOD level refers to the average level between May and November a period when extreme biomass burning cannot occur due to the West African monsoon.

The representative concentration pathway data from the International Institute for Applied Systems Analysis (IIASA) at https://www.iiasa.ac.at/web/home/research/researchPrograms/TransitionstoNewTechnologies/RCP.en.html shows no change in carbonaceous aerosols from the MAF area (Middle East and Africa) before 1950 and then a six fold increase by 2000 with the majority of the increase occurring by 1970. Hence as West Africa is one of the regions where there has been a significant increase it is obvious that the WAP Area background AOD level in 1950 must have been significantly lower than the 1980 level shown in Figure 4. It is therefore possible that this increased background level since 1950 may have also affected the climate of Europe in other seasons and this requires further research.

5.3 Other Aerosol Plumes

Eight continental scale aerosol plumes now exist in the World each year, each in its own season. They can be seen in [Potts, 2017], a poster from the American Geophysical Union Fall Meeting in 2017, available from the Earth and Space Science Open Archive.

My future research on the annual apparitions of anthropogenic, continental scale, aerosol plumes will focus on the seasonal effects of the other plumes on the climate of Europe in summer and autumn, on Australian drought, and on ENSO.

6 CONCLUSIONS

The LME with 1.156 years of data and MERRA-2 with 40 years of data confirm the direct connection between the WAP and the European winter climate in multiple independent ways and my analysis clearly shows that the relationship must be causal.

I therefore conclude that:

1. The hypothesis is proven and that Aerosol Regional Dimming by apparitions of the WAP is the prime trigger for and sustaining influence on the winter climate of Europe driving increased pressure over the MIEA which then creates drought in Iberia, increased rainfall in the UK/Ireland and increased temperatures in northern Europe.

2. The reason that the climate modelling cited in the introduction failed to replicate the significant observed surface pressure rise over the Mediterranean is, of course, that the models did not accurately incorporate the carbonaceous, anthropogenic aerosols of the WAP.

3. The WAP and the other seven continental scale aerosol plumes which now exist each year, each in its own season, must be accurately incorporated in climate models at spatial and temporal resolutions that do not lose the effects of the plumes due to averaging. I suggest a spatial resolution of less than 2° of latitude and longitude and a temporal resolution of less than 1 month are required to do this.

4. With the proof that the WAP changes the climate of Europe 40 to 50 degrees of latitude away it is obviously possible that the other seven continental scale aerosol plumes will have effects which are even more remote from the plume than the WAP is from Europe and this requires investigation.

Finally I concur with *Booth et al.* [2012] that emissions of carbonaceous aerosols are directly addressable by government policy actions and suggest that this is an urgent necessity to restore the winter climate of Europe to its pre-WAP, natural state circa 1950.

7 DATA Sources

The following data was used:

NASA MERRA-2 https://giovanni.gsfc.nasa.gov/giovanni/

NASA Terra https://giovanni.gsfc.nasa.gov/giovanni/

NASA Fire Data https://earthdata.nasa.gov/earth-observation-data/near-real-time/firms/active-fire-data ;

NASA CALIPSO Data https://eosweb.larc.nasa.gov/project/calipso/calipso_table .

NOAA/ESRL images http://www.esrl.noaa.gov/psd/ .

LME https://www.earthsystemgrid.org/

The UK Met Office at https://www.metoffice.gov.uk/weather/learn-about/past-uk-weather-events

The IPCC Reports https://www.ipcc.ch/reports/

Google Earth https://www.google.com/earth/

Forest loss data https://www.globalforestwatch.org/

BP oil production data https://www.bp.com/en/global/corporate/energy-economics/statistical-review-of-world-energy.html

The GGFRP https://www.worldbank.org/en/programs/gasflaringreduction ;

The GVP http://dx.doi.org/10.5479/si.GVP.VOTW4-2013 ;

UN Population Data

https://www.un.org/en/development/desa/population/publications/database/index.asp

8 APPENDIX A - SOURCES OF THE WEST AFRICAN AEROSOL PLUME

The major sources of aerosols in West Africa are biomass burning and gas flares in the oil production industry. Volcanoes are a minor source and are not significant in this region.

8.1 Biomass Burning

Biomass burning in West Africa is a large direct source of carbonaceous aerosols and is part of the traditional annual agricultural cycle. It occurs during the dry season before the start of the local monsoon in April. The level of biomass burning in the region has increased significantly in recent decades and is expected to continue to increase [*Knippertz et al.*, 2015].

In the WAP Area the biomass burning aerosol plume is at its most intense in JFM as Figure 3 shows. The increase in biomass burning in the WAP Area in recent decades has been driven by the increasing population of the WAP Area. The population of West Africa has increased from 71 to 307 million between 1950 and 2010 and is expected to increase to 796 million by 2050. An elevenfold increase in 100 years (United Nations https://www.un.org/en/development/desa/population/publications/database/index.asp). This increasing population has forced: an increase in food production from tropical agriculture with its attendant smoke/aerosols; and increased rainforest clearing to provide living space and agricultural land.

A major source of aerosols in West Africa is forest clearing in Nigeria, the country at the centre of the WAP. Data from The Global Forest Watch at https://www.globalforestwatch.org/ [*Hansen et al.*, 2013] was downloaded and Figure 24 shows the annual forest loss which has trended from under 50,000 Ha in 2001 to 250,000 in 2018 a fivefold increase.

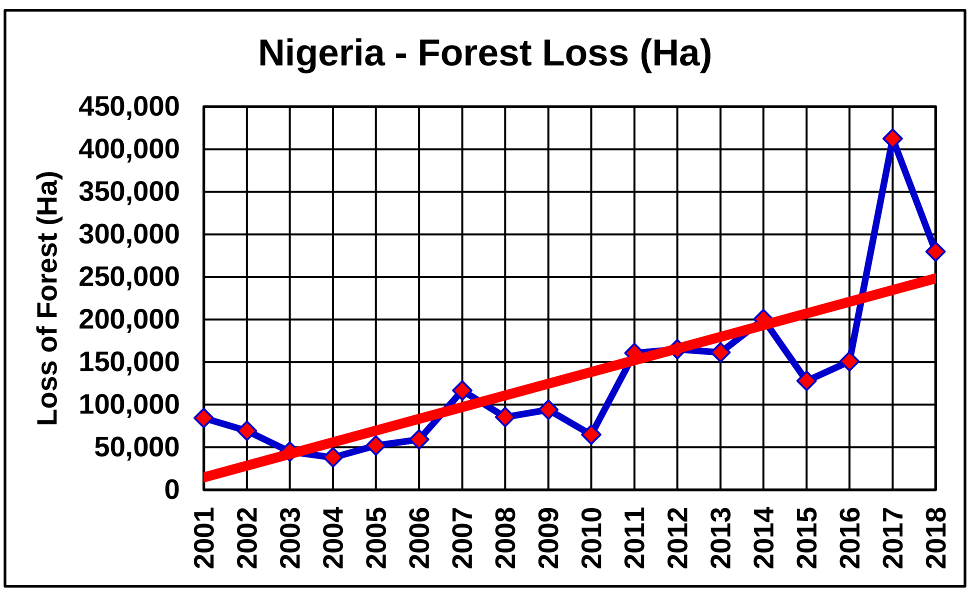

Figure 24: Annual Forest Loss in Nigeria

The archived active fires from Feb 2012 to Feb 2020 from NASA at https://earthdata.nasa.gov/earth-observation-data/near-real-time/firms/active-fire-data was downloaded for the area 5° to 15°N 0° to 10°E. Over 3.8 million observations for this area are included in the database. The data was summed for each day and the daily total then averaged for each month to avoid double counting fires which are recognized on more than one day. The fire data and MERRA-2 AOD are plotted in Figure 25 to show the close connection between fire and AOD in West Africa which is also shown in the high correlation (0.75 significance <0.01) between the AOD and fire numbers in this period.

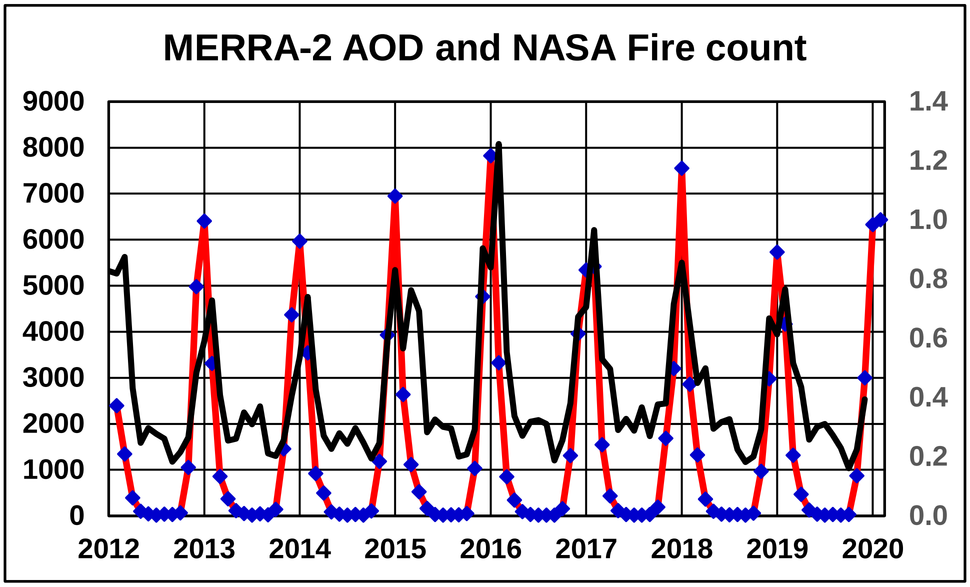

Figure 25: West African Archived Fires (NASA) and NASA MERRA-2 WAP Area AOD.

Together the literature, burned area and fire data show that the extreme AOD in JFM is created by fire in West Africa and the WAP is therefore predominantly carbonaceous.

8.2 Gas Flares

Gas Flares in the oil production industry increased in number over recent decades as oil production in West Africa increased from 274,000 to 2,342,000 barrels of oil per day between 1965 and 2018 (BP Statistical Review of World Energy 2019) with the majority of the increase occurring before 1974. Nigeria is the major producer in the region with 88% of the total oil production in West Africa.

The World Bank has established the GGFRP which estimates Nigeria flares 7.4 billion m^3 of natural gas each year and the gas flare locations are shown in Figure 7. NOAA identifies 359 flare locations in West Africa from Congo to Mauretania with Nigeria hosting the majority at 203. Images of such flares producing aerosols are easily found e.g. Figure 26 from NOAA or at the GGFRP web site.

Figure 26: Gas Flare NOAA at https://ngdc.noaa.gov/eog/viirs/download_global_flare.html

8.3 Volcanoes

The GVP database of volcanic eruptions [*Venzke*, 2013] shows that the WAP Area hosts several volcanoes with only one. Mount Cameroon, recently active with an estimated 18 months of activity since 1900 with volcanic explosivity indices of 1 or 2. As this is unlikely to have any significant impact on the effects discussed in this paper an analysis of volcanic activity has not been included in this paper.

Note: this section on volcanoes is included for completeness as in some regions volcanic activity is a major source of aerosols and a negative finding should be reported.

9 APPENDIX B – CORRELATION MATRIX FOR LME AND MERRA-2

	850	All	Aero	GHG	Land	Orbital	Solar	Volc	MERRA-2	Average
850	1.00	0.03	-0.02	0.02	-0.02	-0.01	0.05	-0.01	-0.12	-0.01
All	0.03	1.00	-0.03	0.01	0.00	-0.02	-0.02	-0.02	0.14	0.01
Aero	-0.02	-0.03	1.00	0.01	-0.07	0.06	-0.09	-0.01	-0.08	-0.03
GHG	0.02	0.01	0.01	1.00	0.02	0.01	-0.03	0.03	0.04	0.01
Land	-0.02	0.00	-0.07	0.02	1.00	-0.01	0.01	-0.03	-0.07	-0.02
Orbital	-0.01	-0.02	0.06	0.01	-0.01	1.00	-0.04	0.03	0.23	0.03
Solar	0.05	-0.02	-0.09	-0.03	0.01	-0.04	1.00	-0.06	0.14	0.00
Volc	-0.01	-0.02	-0.01	0.03	-0.03	0.03	-0.06	1.00	-0.26	-0.04
MERRA-2	-0.12	0.14	-0.08	0.04	-0.07	0.23	0.14	-0.26	1.00	0.00
Average	-0.01	0.01	-0.03	0.01	-0.02	0.03	0.00	-0.04	0.00	0.00

Figure 27: Correlation matrix for LME and MERRA-2 WAP Area AOD/AOD. The average excludes the self-correlations which return 1.00.

Note: There are some small correlations between MERRA-2 AOD and the LME runs however some are positive and some negative in Figure 27 hence the 9 data sets are independent.

ACKNOWLEDGEMENTS

I acknowledge:

NASA: Analyses and visualizations used in this paper were produced with the Giovanni online data system, developed and maintained by the NASA GES DISC; the mission scientists and Principal Investigators who provided the data and images used in this paper including the MERRA-2 data; and Dr Robert Schmunk for the Panoply data viewer;

NASA for the fire data at https://earthdata.nasa.gov/earth-observation-data/near-real-time/firms/active-fire-data ;

NASA for the CALIPSO data obtained from the NASA Langley Research Center Atmospheric Science Data Center at https://eosweb.larc.nasa.gov/project/calipso/calipso_table .

The NOAA/ESRL Physical Sciences Division, Boulder Colorado for the images from their Web site at http://www.esrl.noaa.gov/psd/ .

The CESM1(CAM5) Last Millennium Ensemble Community Project and supercomputing resources provided by NSF/CISL/Yellowstone;

The UK Met Office at https://www.metoffice.gov.uk/weather/learn-about/past-uk-weather-events for the UK flood information;

The IPCC for the images from Assessment Report Four;

Google Earth™ and the copyright holders noted on the image for the image of the Earth;

The United Nations Department of Economic and Social Affairs Population Division for the world population statistics at https://www.un.org/en/development/desa/population/publications/database/index.asp;

The Global Forest Watch at https://www.globalforestwatch.org/ for the forest loss data;

BP for the oil production statistics at https://www.bp.com/en/global/corporate/energy-economics/statistical-review-of-world-energy.html

The Global Gas Flaring Reduction Partnership (World Bank and NOAA) for the gas flare data and image of a flare at https://www.worldbank.org/en/programs/gasflaringreduction ;

The Global Volcanism Program at the Smithsonian Institution for the volcano eruption data. http://dx.doi.org/10.5479/si.GVP.VOTW4-2013 ;

All data supporting the conclusions is available from the sources noted in the text.

This research project was funded personally by the author and his wife Julie.

References

Allen, R. J., S. C. Sherwood, J. R. Norris, and C. S. Zender (2012), Recent Northern Hemisphere tropical expansion primarily driven by black carbon and tropospheric ozone, *Nature*, *485*(7398), 350-354, doi:10.1038/nature11097.

Barry, R. G., and R. J. Chorley (2010), *Atmosphere Weather and Climate* Routledge, Abingdon UK.

Booth, B. B., N. J. Dunstone, P. R. Halloran, T. Andrews, and N. Bellouin (2012), Aerosols implicated as a prime driver of twentieth-century North Atlantic climate variability, *Nature*, *484*(7393), 228-232, doi:10.1038/nature10946.

Cattiaux, J., R. Vautard, C. Cassou, P. Yiou, V. Masson-Delmotte, and F. Codron (2010), Winter 2010 in Europe: A cold extreme in a warming climate, *Geophysical Research Letters*, *37*(20), doi:10.1029/2010gl044613.

Duncan, B. N., I. Bey, M. Chin, L. J. Mickley, T. D. Fairlie, R. V. Martin, and H. Matsueda (2003), Indonesian wildfires of 1997: Impact on tropospheric chemistry, *Journal of Geophysical Research: Atmospheres*, *108*(D15), 4458, doi:10.1029/2002JD003195.

Forster, P., et al. (2007), Changes in Atmospheric Constituents and in Radiative Forcing. In: Climate Change 2007: The Physical Science Basis. Contribution of Working Group I to the Fourth Assessment Report of the Intergovernmental Panel on Climate Change [Solomon, S., D. Qin, M. Manning, Z. Chen, M. Marquis, K.B. Averyt, M.Tignor and H.L. Miller (eds.)] Cambridge University Press, Cambridge, United Kingdom and New York, NY, USA.

García-Herrera, R., D. Paredes, R. M. Trigo, I. F. Trigo, E. Hernández, D. Barriopedro, and M. A. Mendes (2007), The Outstanding 2004/05 Drought in the Iberian Peninsula: Associated Atmospheric Circulation, *Journal of Hydrometeorology*, *8*(3), 483-498, doi:10.1175/jhm578.1.

Gelaro, R., et al. (2017), The Modern-Era Retrospective Analysis for Research and Applications, Version 2 (MERRA-2), *Journal of Climate*, *30*(14), 5419-5454, doi:10.1175/jcli-d-16-0758.1.

Graham, P. W., T. S. Brinsmead, and L. J. Reedman2 (2011), An assessment of competition for biomass resources within the energy and transport sectors*Rep.*, CSIRO.

Hansell, R. A., S. C. Tsay, Q. Ji, K. N. Liou, and S. C. Ou (2003), Surface aerosol radiative forcing derived from collocated ground-based radiometric observations during PRIDE, SAFARI, and ACE-Asia, *Appl Opt*, *42*(27), 5533-5544.

Hansen, M. C., et al. (2013), High-Resolution Global Maps of 21st-Century Forest Cover Change, *Science*, *342*(6160), 850-853, doi:10.1126/science.1244693.

Hegerl, G. C., F. W. Zwiers, P. Braconnot, N. P. Gillett, Y. Luo, J. A. Marengo Orsini, N. Nicholls, J. E. Penner, and P. A. Stott (2007), Understanding and Attributing Climate Change. In: Climate Change 2007: The Physical Science Basis. Contribution of Working Group I to the Fourth Assessment Report of the Intergovernmental Panel on Climate Change [Solomon, S., D. Qin, M. Manning, Z. Chen, M. Marquis, K.B. Averyt, M. Tignor and H.L. Miller (eds.)]. Cambridge University Press, Cambridge, United Kingdom and New York, NY, USA.

Huntingford, C., et al. (2014), Potential influences on the United Kingdom's floods of winter 2013/14, *Nature Clim. Change*, *4*(9), 769-777, doi:10.1038/nclimate2314.

IPCC (2007), IPCC Assessment Report 4 Glossary.

Kalnay, E., et al. (1996), The NCEP/NCAR 40-Year Reanalysis Project, *Bulletin of the American Meteorological Society*, *77*(3), 437-471, doi:10.1175/1520-0477(1996)077<0437:TNYRP>2.0.CO;2.

Kaufman, Y. J., B. N. Holben, D. Tanré, I. Slutsker, A. Smirnov, and T. F. Eck (2000), Will aerosol measurements from Terra and Aqua Polar Orbiting satellites represent the daily aerosol abundance and properties?, *Geophysical Research Letters*, *27*(23), 3861-3864, doi:10.1029/2000GL011968.

Kirchstetter, T. W. (2004), Evidence that the spectral dependence of light absorption by aerosols is affected by organic carbon, *Journal of Geophysical Research*, *109*(D21), doi:10.1029/2004jd004999.

Knippertz, P., M. J. Evans, P. R. Field, A. H. Fink, C. Liousse, and J. H. Marsham (2015), The possible role of local air pollution in climate change in West Africa, *Nature Clim. Change*, *5*(9), 815-822, doi:10.1038/nclimate2727.

Lamarque, J. F., et al. (2010), Historical (1850–2000) gridded anthropogenic and biomass burning emissions of reactive gases and aerosols: methodology and application, *Atmospheric Chemistry and Physics*, *10*(15), 7017-7039, doi:10.5194/acp-10-7017-2010.

Lavers, D. A., and G. Villarini (2013), The nexus between atmospheric rivers and extreme precipitation across Europe, *Geophysical Research Letters*, *40*(12), 3259-3264, doi:10.1002/grl.50636.

Levy II, H., D. T. Shindell, A. Gilliland, M. D. Schwarzkopf, and L. W. Horowitz (2008), Executive Summary in Climate Projections Based on Emissions Scenarios for Long-Lived and Short-Lived Radiatively Active Gases and Aerosols. H. Levy II, D.T. Shindell, A. Gilliland, M.D. Schwarzkopf, L.W. Horowitz, (eds.). A Report by the U.S. Climate Change Science Program and the Subcommittee on Global Change Research, Washington, D.C.

Luterbacher, J., M. A. Liniger, A. Menzel, N. Estrella, P. M. Della-Marta, C. Pfister, T. Rutishauser, and E. Xoplaki (2007), Exceptional European warmth of autumn 2006 and winter 2007: Historical context, the underlying dynamics, and its phenological impacts, *Geophysical Research Letters*, *34*(12), doi:10.1029/2007gl029951.

McGregor, G. R., and S. Nieuwolf (1977), *Tropical Climatology*, 207 pp., John Wiley and Sons.

Menon, S., J. Hansen, L. Nazarenko, and Y. Luo (2002), Climate Effects of Black Carbon Aerosols in China and India, *Science*, *297*(5590), 2250-2253, doi:10.1126/science.1075159.

Novakov, T., V. Ramanathan, J. E. Hansen, T. W. Kirchstetter, M. Sato, J. E. Sinton, and J. A. Sathaye (2003), Large historical changes of fossil-fuel black carbon aerosols, *Geophysical Research Letters*, *30*(6), 1324, doi:10.1029/2002GL016345.

Oluleye, A., K. O. Ogunjobi, A. Bernard, V. O. Ajayi, and A. A.A. (2012), Multiyear Analysis of Ground-Based Sunphotometer (AERONET) Aerosol Optical Properties and its Comparison with Satellite Observations over West Africa, *Global Journal of HUMAN SOCIAL SCIENCE Geography & Environmental GeoSciences*, *12*(10).

Osborn, T. J. (2004), Simulating the winter North Atlantic Oscillation: the roles of internal variability and greenhouse gas forcing, *Climate Dynamics*, *22*(6-7), doi:10.1007/s00382-004-0405-1.

Ott, L., B. Duncan, S. Pawson, P. Colarco, M. Chin, C. Randles, T. Diehl, and E. Nielsen (2010), Influence of the 2006 Indonesian biomass burning aerosols on tropical dynamics studied with the GEOS-5 AGCM, *Journal of Geophysical Research: Atmospheres*, *115*(D14), D14121, doi:10.1029/2009JD013181.

Otto-Bliesner, B. L., E. C. Brady, J. Fasullo, A. Jahn, L. Landrum, S. Stevenson, N. Rosenbloom, A. Mai, and G. Strand (2016), Climate Variability and Change since 850 CE: An Ensemble Approach with the Community Earth System Model, *Bulletin of the American Meteorological Society*, *97*(5), 735-754, doi:10.1175/bams-d-14-00233.1.

Potts, K. A. (2017), Poster: The South East Asian Aerosol Plume: The Cause of All El Niño Events, in *AGU 2017 Fall Meeting*, edited, Earth and Space Science Open Archive (ESSOAr, New Orleans, USA, doi:https://doi.org/10.1002/essoar.10500075.1.

Ralph, F. M., and M. D. Dettinger (2011), Storms, floods, and the science of atmospheric rivers, *Eos, Transactions American Geophysical Union*, *92*(32), 265-266, doi:10.1029/2011EO320001.

Ramanathan, V. (2006), ATMOSPHERIC BROWN CLOUDS: HEALTH, CLIMATE AND AGRICULTURE IMPACTS, *Scripta Varia 106*.

Remer, L. A., et al. (2009), Executive Summary, in Atmospheric Aerosol Properties and Climate Impacts, A Report by the U.S. Climate Change Science Program and the Subcommittee on Global Change Research [Mian Chin, Ralph A. Kahn, and Stephen E. Schwartz (eds.)]. National Aeronautics and Space Administration, Washington, D.C., USA.

Remer, L. A., et al. (2005), The MODIS Aerosol Algorithm, Products, and Validation, *Journal of the Atmospheric Sciences*, *62*(4), 947-973, doi:10.1175/JAS3385.1.

Schaller, N., et al. (2016), Human influence on climate in the 2014 southern England winter floods and their impacts, *Nature Clim. Change*, *6*(6), 627-634, doi:10.1038/nclimate2927 http://www.nature.com/nclimate/journal/v6/n6/abs/nclimate2927.html#supplementary-information.

Seifkar, N., X. Lu, M. Withers, R. Malina, R. Field, S. Barrett, and H. Herzog (2015), Biomass to Liquid Fuels Pathways*Rep.*

Solomon, S., et al. (2007), Technical Summary. In: Climate Change 2007: The Physical Science Basis. Contribution of Working Group I to the Fourth Assessment Report of the Intergovernmental Panel on Climate Change [Solomon, S., D. Qin, M. Manning, Z. Chen, M. Marquis, K.B. Averyt, M. Tignor and H.L. Miller (eds.)]. Cambridge University Press, Cambridge, United Kingdom and New York, NY, USA.

Sterl, A., C. Severijns, H. Dijkstra, W. Hazeleger, G. Jan van Oldenborgh, M. van den Broeke, G. Burgers, B. van den Hurk, P. Jan van Leeuwen, and P. van Velthoven (2008), When can we expect extremely high surface temperatures?, *Geophysical Research Letters*, *35*(14), doi:10.1029/2008gl034071.

van Oldenborgh, G. J., S. Drijfhout, A. van Ulden, R. Haarsma1, A. Sterl, C. Severijns, W. Hazeleger, and H. Dijkstra (2009), Western Europe is warming much faster than expected, *Climate of the Past*, *5*, 1 - 12.

Venzke, E. (2013), Volcanoes of the World v. 4.4.3, edited by S. I. G. V. Program, doi: http://dx.doi.org/10.5479/si.GVP.VOTW4-2013.

Vicente-Serrano, S. M., and J. I. López-Moreno (2006), The influence of atmospheric circulation at different spatial scales on winter drought variability through a semi-arid climatic gradient in Northeast Spain, *International Journal of Climatology*, *26*(11), 1427-1453, doi:10.1002/joc.1387.

Wang, C. (2004), A modeling study on the climate impacts of black carbon aerosols, *Journal of Geophysical Research: Atmospheres*, *109*(D3), D03106, doi:10.1029/2003JD004084.

Winker, D. M., M. A. Vaughan, A. Omar, Y. Hu, K. A. Powell, Z. Liu, W. H. Hunt, and S. A. Young (2009), Overview of the CALIPSO Mission and CALIOP Data Processing Algorithms, *Journal of Atmospheric and Oceanic Technology*, *26*(11), 2310-2323, doi:10.1175/2009jtecha1281.1.

Yiou, P., R. Vautard, P. Naveau, and C. Cassou (2007), Inconsistency between atmospheric dynamics and temperatures during the exceptional 2006/2007 fall/winter and recent warming in Europe, *Geophysical Research Letters*, *34*(21), L21808, doi:10.1029/2007GL031981.

Young, A. M., K. T. Skelly, and J. M. Cordeira (2017), High-impact hydrologic events and atmospheric rivers in California: An investigation using the NCEI Storm Events Database, *Geophysical Research Letters*, *44*(7), 3393-3401, doi:10.1002/2017GL073077.

Zhang, R., et al. (2013), Have Aerosols Caused the Observed Atlantic Multidecadal Variability?, *Journal of the Atmospheric Sciences*, *70*(4), 1135-1144, doi:doi:10.1175/JAS-D-12-0331.1.